Accepted Manuscript

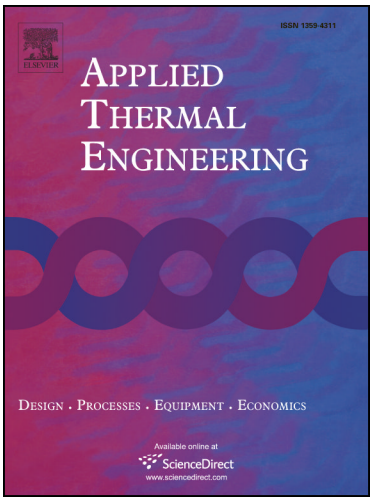

Research Paper

Cold recovery from LNG-regasification for polygeneration applications

Antonio Atienza-Márquez, Joan Carles Bruno, Alberto Coronas

PII: S1359-4311(17)36614-0
DOI: https://doi.org/10.1016/j.applthermaleng.2017.12.073
Reference: ATE 11594

To appear in: *Applied Thermal Engineering*

Received Date: 15 October 2017
Revised Date: 14 December 2017
Accepted Date: 20 December 2017

Please cite this article as: A. Atienza-Márquez, J. Carles Bruno, A. Coronas, Cold recovery from LNG-regasification for polygeneration applications, *Applied Thermal Engineering* (2017), doi: https://doi.org/10.1016/j.applthermaleng.2017.12.073

Cold recovery from LNG-regasification for polygeneration applications

Antonio Atienza-Márquez *, Joan Carles Bruno, Alberto Coronas

Universitat Rovira i Virgili, CREVER – Group of Applied Thermal Engineering, Mechanical Engineering Department, Av. Països Catalans 26, 43007 Tarragona, Spain

*Corresponding author: antonio.atienza@urv.cat

Abstract

Liquefied Natural Gas (LNG) has a high exergetic potential because of its low temperature (around -162^{o}C), although usually the cold released from LNG regasification is wasted. In this paper, the LNG supply chain and the conventional regasification technologies are reviewed and analyzed to identify the cold recovery opportunities. Also, an overview of the applications and technologies for LNG cold recovery is presented. Although there many applications and technologies for this purpose, most of them are immatures and their implementation is not widespread. Besides, most of the literature is focused on exploiting LNG cold for a single application, while LNG cold offers a lot of possibilities of exploitation via polygeneration. In the second part of this paper, a polygeneration plant for power and cold production is proposed and modelled as a case study for cold recovery from LNG-regasification. The structure of the plant is engineered to operate with high flexibility. The LNG exergy is exploited in cascade for power production and cold generation in a district cooling network with three different temperature levels. The plant achieves an equivalent energy saving of 81.1 kWh/ton-LNG with an exergetic efficiency of 34.7%. The seawater consumption is reduced 67.6% respect to the typical LNG regasification.

Keywords: Liquefied Natural Gas regasification; Exergy recovery; Polygeneration; Combined cold and power production; Performance indicators

1. Introduction

Natural gas (NG) is the fossil fuel with the lowest carbon footprint and the most clean combustion [1–3]. At present, NG accounts approximately a quarter of world primary energy

supply [4] and its demands is estimated to grow 1.6% per annum between 2016 and 2035, being the only fossil fuel whose demand prediction increases [5]. In fact, natural gas is forecast to be the most important source of primary energy supplied towards 2050 [6].

The unequal distribution of NG reserves makes its transport a constraint. Usually, NG is transported by pipeline. However, when the distance between the importer country and the gas suppliers is too long, the only feasible solution is NG liquefaction [7] and its transport by ship in its cryogenic form: Liquefied Natural Gas (LNG). Additionally, the transport as LNG is more flexible for the gas market and avoids the energy dependency from a specific country. In 2015, LNG represented near 10% of the global primary energy demand [8,9]. Furthermore, the importance of LNG in the energy mix is increasing. At present, LNG trade means 32% of the total NG trade and this percentage will reach 50% by the year 2035 [5].

LNG has to be regasified before supplying it to the end-users (industry clusters, electrical power plants, residential and office buildings, hotels, etc.). Nowadays, the number of LNG receiving facilities in operation worldwide is more than one hundred (see **Fig. 1 (a)**) with a regasification capacity near to 800 millions of tons (MT), and 19 receiving facilities are under construction (most of them in China and India) [8]. **Figure 1 (b)** shows the amount of LNG exported and imported in 2016 by the top countries in the LNG market. In 2016, the global LNG trade reached 258 MT [8]. Qatar and Japan highlight as the leader countries in the LNG landscape as the main exporter and importer respectively.

Fig. 1. World map with: (a) Worldwide distribution of LNG regasification plants and major regasification capacities (in million tons per annum - MTPA) and (b) the most remarkable amounts of LNG in MTPA exported or imported in 2016 by the main countries in LNG market and. Source [8].

At present, several international projects that aim to promote the use of LNG as primary energy are in progress. For instance, the project "*CORE LNGas hive*" (co-financed by the European Union) aims to promote LNG as fuel for transport in maritime sector of the Iberian Peninsula [10]. Also, the project "*HDgas*" (Horizon 2020 European program) is focused on the use of LNG as fuel for heavy vehicles like trucks [11]. On the other hand, projects such as "*CryoHub*" [12] (Horizon 2020 European program) are an evidence of the interest in cryogenic fluids. The scope of this project is the large-scale cryogenic storage and use of cryogenics fluids to be used in the agro-food sector.

Besides, the very low temperature of LNG (-162^{o}C) makes it a "gold mine" from the exergetic point of view. In fact, the temperature of cold focus is crucial for the thermal efficiency of thermodynamic cycles, even more than the hot focus. This is clearly shown in **Figure 2** where are compared two thermal machines with the same Carnot's efficiency but operating between different temperatures. The cycle whose cold focus is at the temperature of LNG requires a much lower temperature difference with respect to the ambient than the other cycle to achieve the same Carnot's efficiency. Thus, the variation of 1^{o}C below the ambient affects much more the thermal efficiency than the variation of 1^{o}C above the ambient.

Fig. 2. Two thermal cycles with the same Carnot's efficiency and operating between different temperatures.

The objective of this paper is to showcase the relevance of cold recovery from LNG-regasification for polygeneration applications. We analyze the LNG supply chain not only to understand why the recovery of cold from LNG-regasification is important, but also to identify the cold recovering opportunities. Also, an overview of the existing literature about applications and technologies for cold recovery from LNG-regasification is presented. Finally, we propose and analyze a polygeneration plant where LNG is regasified and its exergy is exploited in a District Cooling (DC) network and also for electric power generation.

2. LNG supply chain: Regasification as cold recovery opportunity

The regasification is only one of the multiple stages of NG's supply chain. **Figure 3** illustrates the main stages involved in the LNG supply chain. Before being liquefied at the liquefaction plant, the raw gas extracted has to be submitted to several treatment processes to meet with its chemical composition limits [3]. Solids, mercury, water, acid gas, heavy hydrocarbons and non-hydrocarbons such as nitrogen or helium have to be removed. The natural gas liquefaction is a process that requires an important amount of energy (300-850 kWh/ton-LNG depending on the liquefaction technology used [13,14]). The NG liquefaction process technologies differ from each other depending on the type of refrigerants used, the number of refrigerant cycles, cascade or parallel arrangement of the refrigeration cycle, etc. [15]. At the end of the liquefaction process, the temperature of the LNG is approximately -162^{o}C with a density of 400-500 kg m^{-3} and its physical volume is around 1/600 the volume of NG [2].

Fig. 3. A block diagram of the LNG supply chain.

LNG is transported over long distances in carriers of auto-refrigerated LNG tankers with a storage capacity up to 266,000 m^3 of LNG [16]. Once the LNG tanker docks at the receiving terminal port, the LNG is unloaded from the carrier to the terminal tanks. For instance, the regasification plant of Barcelona (Spain) has total storage capacity of 760,000 m^3 of LNG (four tanks of 150,000 m^3 and two of 80,000 m^3) [17]. Inside LNG tanks, some boil-off gas (BOG) is produced. The management of the boil-off gas is an important task to control the pressure inside tanks between 110-250 mbar(g) [18]. The BOG is compressed and re-liquefied in the recondenser mixed with the LNG that is pumped from the tanks. Alternatively, the BOG may be introduced in the carriers of LNG tankers through a vapor line or it may be burned in a torch.

Next, the LNG leaving the recondenser is pumped to the vaporizers where the regasification occurs. Among the different types of vaporizer technologies (submerged combustion vaporizer – SCV, ambient air vaporizer – AAV, intermediate fluid vaporizer – IFV or shell and tube vaporizer – STV), open rack vaporizers (ORVs) (**Fig. 4 (a)**) are the most widely used due to a high thermal efficiency, low operational cost, simple operability, etc. [19]. The basic working principle of these vaporizers (and also for super ORVs [20]) is the following. The main LNG stream is divided into several streams that flow upward inside metallic tubes arranged in panels. The seawater used as heat source is pumped and it falls from the top side of the vaporizer and flows downward in contact with the outer surface of the tubes. By this way, the temperature of LNG increases up to 5-10^{o}C, so it is regasified. However, the cold seawater leaving the vaporizer returns back to the sea without any useful application. This fact not only represents a waste of energy of around 200-230 kWh/ton-LNG regasified [13] and an energy consumption by seawater pumps of ~8 kWh/ton-LNG [21], but this also represents an environmental impact on marine sea life [22,23].

Fig. 4. The most common vaporizer technologies to regasify LNG: (a) Open rack vaporizer – ORV, (b) Intermediate fluid vaporizer – IFV, (c) Submerged combustion vaporizer – SCV.

IFVs are an alternative to ORVs (**Fig. 4 (b)**). These vaporizers are similar to shell-and-tube heat exchangers [24]. An intermediate fluid (mainly propane) vaporizes and condenses inside a tank where the condenser (LNG side) and evaporator (heat source side) are located. Thus, heat is transferred from the heat source fluid (mainly seawater) to the LNG indirectly to prevent the

solidification of the hot source fluid. The intermediate fluid vaporizes taking heat from the heat source. In the condenser, the LNG is regasified by absorbing the latent heat of condensation released by the intermediate fluid. Finally, the NG is heated up to the required temperature in the thermolator. The use of IFV is quite attractive because it allows the use of alternative fluids rather than seawater as heat source to regasify LNG [25]. If the fluid used as heat source in the vaporizer has adequate heat transfer fluid properties, the cold could be transported from the vaporizer (regasification site) to potential "cold consumers". For instance, in D. Pineda Quijano et al. [26] the same CO_2 stream used as heat source fluid in an IFV is also used as heat transfer fluid to transport the cold from a LNG regasification plant to "cold consumers".

On the other hand, SCVs (**Fig. 4 (c)**) often operate as a support for the ORVs or IFVs to cover peak shaving in regasification demand or to ensure the regasification demand in emergency situations. SCVs use the combustion heat of a fuel (diesel, NG or even BOG) to regasify the LNG [27]. LNG flows inside a serpentine coil submerged in a water bath that receives the heat from the combustion gases [28]. If NG is used as fuel, a fraction of the LNG is consumed in the combustion chamber (~2% [29]) and the cold of LNG is rejected to the ambient via the exhaust gases.

Therefore, LNG regasification represents the best opportunity to recover part of the energy supplied at the liquefaction stage. But, if such a high amount of cold can be recovered, why this cold is wasted in most of the LNG regasification plants worldwide? Actually, the interest in exploiting LNG cold exists but there are some important technical and non-technical barriers to overcome:

- Usually "cold consumers" are far away from the LNG regasification plants.
- Shortage of heat transfer fluids with suitable thermal properties, low price, safe, and climate-friendly to transport the cold from the regasification plant to the end-users.
- Insufficient and fluctuating cold demand in many cases.
- Mistrust among "cold consumers" to substitute their refrigeration systems by new systems designed to exploit cold recovered from LNG-regasification.
- Companies managing LNG regasification plants have limited interest in providing energy services other than NG to third parties. Thus, certain collaboration with others is required.

So far, these barriers have blocked a further development of technologies for LNG cold recovery. However, this scenario is changing. As a result of recent agreements in climate

change policy (e.g., Paris Agreement 2015 [30]), institutions such as the European Commission are pointing out industrial waste heat and cold recovery, and particularly cold recovery from LNG-regasification, a crucial task to reduce greenhouse gases emissions [31]. Furthermore, the cold recovered from LNG-regasification contributes to accomplish other important objective to mitigate global warming and to attain a greener refrigeration system by replacement of traditional refrigeration systems: global warming potential (GWP) refrigerants phase-out [32]. This fact benefits "cold consumers" because they can avoid paying taxes on GWP refrigerants. Hence, the LNG cold recovering is not only interesting from an energetic point of view, but also from an environmental and economic perspective.

3. LNG cold recovery: An overview of technologies and applications

Although in the conventional regasification process the LNG cold is not recovered, the high exergy content of LNG is very attractive to be exploited in multiple industrial activities and low temperature processes. **Figure 5** shows the temperature level of several low-temperature applications that are suitable for exploiting LNG exergy. Some of most studied applications of LNG exergy are: cryogenic power generation, air separation process, CO_2 capture or seawater desalinization [33]. Others less explored applications are light and heavy hydrocarbon separation [34,35], cold storage [36], etc.

Fig. 5. Temperature levels for several applications that can use the cold from LNG-regasification.

The joint implementation of some of the LNG cold recovery applications listed above might benefit from the implementation of polygeneration plants. These plants are characterized by the production of multiple energy services using highly energy integrated processes and simultaneously using several primary energy sources. Next, we give an overview of the existing literature about the main technologies and applications for exploiting LNG exergy.

3.1. LNG cold use in electric power cycles

The use of LNG cold to enhance the thermal efficiency of thermal power plants is the most studied application in the literature. LNG thermal exergy is used as heat sink in the condenser of Rankine cycles (RCs) or Kalina cycles, to reduce the temperature of air entering the compressor

of Brayton cycles (BCs), etc. Additionally, LNG mechanical exergy may be converted into electricity by direct expansion. Romero Gómez et al. [37] described in detail different types of power plants configurations to exploit LNG exergy. On the other hand, in order to be able to compare the efficiencies of the power cycles of the papers reviewed below using the same reference basis, we use a common performance indicator defined as the ratio between the electric power output of the system and the regasified LNG mass flow rate given in kWh/ton-LNG.

RCs are convenient for a wide range of low temperature heat sources (seawater, low-grade waste heat, solar energy, geothermal energy, etc.). **Figure 6** summarizes a combination of the most common RCs. For example, Ferreira et al. [38] compared the energy saving of the regasification plant of Sines (Portugal) when it is upgraded with (1) a LNG direct expansion unit, (2) a simple RC cycle and (3) the combination of both. They determined that the plant produces a net power of 2 MW (13.6 kWh/ton-LNG) when using LNG as heat sink in a simple RC using propene as working fluid (operating between 842.03-95.99 kPa) and seawater as heat source. The increase in the net power by adding a LNG direct expansion unit to the simple RC was negligible. Ahmadi et al. [39] simulated a transcritical CO_2 basic RC using geothermal water at 140^{o}C as heat source in the base case. LNG was firstly used as heat sink to condense the CO_2. LNG was regasified using water at ambient temperature as heat source and expanded in a turbine to produce extra power. For the base case (CO_2 entering the turbine at 12 MPa), the net power of the plant was around 540 kW (44 kWh/ton-LNG) with a exergetic efficiency of around 12%. Furthermore, regenerative RCs are a modification of the basic RC to reduce the heat rejection in the condenser [40].

Fig. 6. Typical power cycle configurations: (a) LNG direct expansion; (b) combined Rankine power cycle type I; (c) combined Rankine power cycle type II.

Combined RCs have been also studied. In **Fig.6**, we differentiate between combined Types I and II, depending on how the cycle is arranged. Oliveti et al. [41] studied two cascaded ORCs with LNG direct expansion. This combined cycle has a Type I structure (**Fig. 6**) which is suitable for heat sources at high temperatures. The top cycle is a steam RC (vaporizing at 4 MPa and condensing at 0.013 MPa) driven by waste heat at 400^{o}C from an incineration plant located close to the planned Gioia Tauro LNG regasification plant (Italy). The bottoming RC uses ammonia as working fluid (vaporizing at 0.4 MPa and condensing at 0.04 MPa) and it exploits the LNG cold in the condenser. The proposed plant produced 27.8 MW for a LNG flow rate of

97 kg s^{-1} (79.6 kWh/ton-LNG) with a thermal efficiency of 28.8%. In addition, the seawater flow rate was reduced 60% respect to the regasification plant without LNG cold recovery. As an example of combined RCs type II, Ferreiro García et al. [42] presented a regasification and power plant that consists of two cascade transcritical ORCs using argon (higher and lower pressures of 21.7 MPa and 3.91 MPa, respectively) and methane (higher and lower pressures of 19.1 MPa and 4.0 MPa, respectively) as working fluids and a multi-stage direct expansion unit. The heat source of both RCs is seawater. This plant has a net power of 65.3 kWh/ton-LNG and a thermal and exergetic efficiencies of 24.1% and 42.7%, respectively.

Brayton cycles (BCs) are suitable for high temperature heat sources (e.g., combustion heat) [37]. In open BCs, the most straightforward uses of LNG cold are focused on the reduction of the compression work: air cooling at the compressor inlet or intercooling for multiple stage compression. Shi et al. [43] presented a power plant where both LNG cold uses were applied. The mirror gas-turbine technology is a solution to cool the exhaust gasses and increase the useful work [44]. On the other hand, LNG exergy can be exploited as heat sink in closed BCs.

Dispenza et al. [45,46] presented a regasification and power plant that consists of an open BC and a closed BC. LNG was used as heat sink in the closed BC. The exhaust gases leaving the open BC are used as heat source of the closed BC (with He as working fluid). The higher and lower temperatures of He in the closed BC were 579^{o}C and -129^{o}C, respectively; and the higher and lower pressures were 2.27 MPa and 0.3 MPa, respectively. The power capacity of the plant was 380 kWh/ton-LNG. The thermal efficiency of the plant was 69% (considering the heat absorbed by LNG as a useful output of the plant) and the exergetic efficiency was 49% (considering the exergy of regasified NG supplied to the distribution pipeline as a useful exergy output of the plant). Morosuk and Tsatsaronis [47] discussed the convenience of installing a LNG direct expansion unit in a LNG regasification and power plant that combined an open and a closed BC. The closed BC (working with N_2 between 4275 kPa and 285 kPa) was driven by the combustion gases leaving the open BC (435^{o}C) and it used LNG as heat sink. The regasification capacity of the plant increased without a LNG direct expansion unit while the electric power output remains near the same. The power capacity of the plant was 144 MW (531 kWh/ton-LNG) with a thermal efficiency of 78.1% (considering the heat absorbed by LNG as a useful output of the plant) and an exergetic efficiency of 52.1% (considering the difference in mechanical exergy between NG regasified and the LNG storage as a useful exergy output of the system).

The combination of RCs with BCs is a further option. Romero Gómez et al. [48] presented a combined power plant that consists of a closed BC and a RC in series. LNG exergy is exploited as cooling media in the compressor suction of the closed BC. The heat source of the closed BC is combustion heat at 1300ºC. Once the combustion gases have feed the closed BC, they are used as heat source in the RC. The most advantageous working fluids were He and CO_2 for the BC and the RC, respectively. The plant produced 2.465 MW/kg s^{-1} LNG regasified (684.7 kWh/ton-LNG) with a thermal efficiency of 67.6%. Lu and Wang [49] studied a regasification and power plant that combined an open BC, ammonia-water RC (optimal higher and lower pressures are 2.29 MPa and 0.04 MPa, respectively) and LNG direct expansion unit. LNG is also used as heat sink in the condenser of the RC. The maximum temperature in the plant was 993.2ºC. The optimal net power of this plant was 48.3 MW (around 139 kWh/ton-LNG).

Other thermal power cycles have been explored in the literature. For instance, Kalina cycles (KCs) have a structure similar to ORCs but with a solution circuit and higher exergetic efficiencies [19]. KCs use a mixture with different boiling points as working fluid. As an example of systems operating with mixtures as working fluids, Miyazaki et al. [50] modelled a plant that consist of an ammonia-water power cycle driven by heat from an incinerator and a LNG power cycle. The plant has a power production of 105 kWh/ton-LNG with a thermal efficiency of 29% and an exergetic efficiency of 30% (considering the exergy of the regasified NG supplied to the distribution pipeline as an output). On the other hand, Wang et al. [51] proposed a thermoacoustic Stirling generator to produce electricity from LNG cold.

The literature survey presented above reveals that the definitions of both the thermal and exergetic efficiencies are heterogeneous. The thermal efficiency is mainly defined as the ratio of the power produced by the system to the heat input from the heat sources [40–42,48–50]. However, there are some authors that also consider the heat absorbed by the LNG during the regasification process as a useful output of the power plant [46,47]. With respect to the exergetic efficiency, there are authors that only consider the electricity output of the system as a useful exergy output of the power plant [39,40,42], while others also consider the exergy of regasified NG supplied to the distribution pipeline [46,50] or the difference in mechanical exergy between the NG regasified and the LNG storage in tanks [47].

3.2. Cryogenic air separation

Cryogenic air separation is an appropriate technology when aiming to obtain high purity oxygen, argon and nitrogen from air. This separation process is carried out in air separation units (ASUs) where very low temperatures are required (-173^{o}C to -193^{o}C). Thus, LNG can be integrated in the air separation process to reduce energy consumption of the refrigeration system. As the operating temperatures of cryogenic ASUs are lower than LNG temperature (-162^{o}C), LNG cold can be recovered efficiently [52].

Ebrahimi and Ziabasharhagh [53] studied a two columns cryogenic ASU where LNG cold was integrated and recovered. The LNG integration in the ASU contributed to an energy saving of 8.04%. The oxygen production rate of the plant was 68.5 ton/h (~0.24 kg-O_2/kg-LNG). Merhpooya et al. [54] simulated a polygeneration plant where cold recovered from LNG-regasification was applied in (1) a double-column ASU to produce high purity O_2 and N_2, (2) in a coal gasification process, (3) as heat sink for a transcritical CO_2 power generation cycle and (4) in a cryogenic CO_2 capturing system. The plant produced an electric power generation of 11.5 MW (~95 kWh/ton-LNG) and an oxygen production of 79.5 ton/h (~0.66 kg-O_2/kg-LNG).

3.3. Seawater desalination

Freeze desalination (FD) is an alternative to the common technologies for seawater desalination (reverse osmosis, multi-effect distillation, multistage-flash, etc.). FD consists basically of lowering the temperature of seawater to its crystallization point with the aim to produce ice crystals that, by nature, are mostly composed of pure water. To use LNG cold is a solution to decrease the input of electrical energy required by the refrigeration systems used in FD.

Although FD is an immature desalination technology, some authors are simulating and developing experimental prototypes to evaluate the performance for future implementation in industry. Cao et al. [55] simulated a flake ice-maker that uses an intermediate refrigerant to transfer the cold from LNG to seawater. The device produces 2 kg-ice melt water/kg-LNG with energy consumption near null. Lin et al. [56] built a seawater FD prototype that exploit LNG cold and using R410A as intermediate refrigerant between LNG and seawater in an flake-ice maker. The experiments carried out reported 2 kg-fresh water/kg-LNG and the desalination rate was 50%. Xie et al. [57] developed a direct contact ice generator prototype that allows to exploits LNG cold and to regasify LNG simultaneously using HFE-7100 as intermediate refrigerant. The ice production efficiency was 0.92-1.15 kg-ice/kg-LNG and the desalination rate was 83.5-80.1%.

3.4. Agro-food industry and commercial sector

Only a few works deal with the use of cold energy for agro-food industry or commercial sector. La Rocca [58,59] analyzed the cold recovering from LNG-regasification for deep-freezing in agro-food factories and for air-conditioning in supermarkets and hypermarkets using CO_2 as secondary fluid. For this purpose, the author uses a modular LNG regasification unit proposed by Dispenza et al. [60] with a LNG regasification capacity of 62.7 kg h^{-1}. The total cooling demand (at -43ºC) from the agro-food cluster analyzed was 9 MW and the global energy and exergy efficiencies for the agro-food cluster were 95% and 79%, respectively. In the case of the analyzed hypermarket, the cooling demand was 6 MW (0.5 MW at -35ºC and 5.5 MW at -15ºC) with a global energy and exergy efficiencies of 87% and 76%, respectively. Also, Messineo and Panno [61] aimed to exploits the LNG cold in an agro-food industry near to the regasification site in Sicily (Italy) using CO_2 as heat transport fluid.

4. Case study: polygeneration plant for LNG cold recovery

From the previous review it is clear that the recovery of cold from LNG regasification is a very promising technology to provide multiple energy services. However, the LNG cold recovery in regasification terminals is not widespread. At present, the few regasification facilities where LNG cold is recovered are mostly located in Japan where this LNG cold is mainly used to produce power in RC and direct expansion units and also for air separation processes [37]. In the next section, a case study is presented as an example in order to better quantify the potential benefits of this innovative application.

4.1. Description of the polygeneration plant

Figure 7 shows a schematic diagram of the polygeneration plant for LNG cold recovery proposed in this work. This plant is an example of LNG cold recovery integration in an actual regasification facility. The aim is to replace one of the ORV (with a regasification capacity of 150,000 Nm^3 h^{-1}) that operates in the LNG regasification plant of Barcelona by a system that exploits the LNG cold exergy. The Barcelona LNG terminal is located in the port of Barcelona (41.33º N, 2.16º E), Spain. Currently, it has a rated regasification capacity of 1,950,000 Nm^3 h^{-1} with 13 ORVs and 2 SCVs installed [62]. This LNG facility is a promising scenario for

planning a system that recovers the cold from LNG-regasification because of the existence in the vicinity of the regasification site of an industrial area with a huge cold demand throughout the year.

Fig. 7. Schematic diagram of the polygeneration plant for cold recovery from LNG-regasification.

The proposed polygeneration plant gives the following services: LNG regasification ready for the transport network, district cooling service at three different temperature levels and electric power. LNG regasification is a compulsory service of the plant. The plant is divided into four operational blocks (or subsystems) which are able to operate independently with high flexibility. The LNG exergy is exploited as follows:

- A transcritical RC (RC-1) with regeneration using argon as working fluid. LNG and seawater are used as heat sink and heat source respectively. This power cycle is designed for operating upstream of the district cooling network with the aim to take advantage of the low temperature of LNG leaving the pump P1, which is much lower than the required by the "cold consumers" connected to the district cooling network.

- A District Cooling (DC) network using CO_2 as heat transport fluid. The DC network provides cooling at three temperature levels: The low-temperature DC network (LT-DC) provides refrigeration to cold chambers, refrigerated warehouses, etc.; the medium-temperature DC network (MT-DC) to commercial centers (e.g., hypermarkets); and the high-temperature DC network (HT-DC) to residential and office buildings, hotels, etc. Moreover, the DC network is combined with a power generation cycle (RC-2) which is driven by low-grade waste heat from, e.g., auxiliary equipment such as cooling towers.

- A transcritical CO_2 RC (RC-3) with regeneration and intermediate reheating. This power cycle uses LNG as heat sink. It is designed for operating downstream of the DC network + RC-2 in order to exploit the temperature of LNG that still is much lower than the ambient temperature. On the other hand, the heat generated in a biomass boiler of 10 MW is used as heat source. At present, a biomass thermal power plant is in operation nearby the regasification site.

- A LNG direct expansion unit (EXP). The pressure of the supplied NG has to be adapted because the distribution pipeline pressure is lower than the operating pressure of the regasification plant. Thus, EXP harnesses the exergy released in the expansion.

4.2. Operation of the polygeneration plant

The structure of the plant is engineered to exploit the LNG cold exergy in cascade. The plant operates as follows. Once the LNG leaves the BOG recondenser (stream 1), it is pressurized to high pressure by the pump P1 (stream 2). In a first step, LNG is used as heat sink of RC-1 to condense the working fluid (Ar) (stream 11) in the condenser C-1. Argon has been selected has working fluid for RC-1 because it is a climate-friendly and natural fluid with a freezing point (-189.34^{o}C) lower than the LNG temperature. Hence, the pinch-point temperature difference in C-1 can be reduced as much as possible without crystallization risk. The Ar is pressurized by P2, heated in the seawater heater H-1 and expanded in the turbine T1 to produce electricity.

The LNG downstream leaving C-1 (stream 3) is used in the condenser C-2 to condense the CO_2 (stream 17) selected as heat transport fluid of the DC network. CO_2 is much less viscous than other fluids such as glycol water at low temperatures. Also, it is environmentally-friendly, secure and cheap so that it is a good candidate for the DC network. However, its freezing point (-56.5^{o}C) is above the LNG temperature and this implies a risk of crystallization. In this sense, the benefit of the power cycle RC-1 is twofold: It not only produces electrical energy, but also it contributes to increase the temperature of LNG at the entrance of CD-2 (stream 3). Thus, the pinch temperature difference in CD-2 can be reduced with a minor CO_2 crystallization risk. The liquid CO_2 at -50^{o}C is pumped by P3 and supplied to the "cold consumers", who are connected in parallel with the DC network. Both LT-DC and MT-DC users operate with ammonia as secondary refrigerant inside their facilities, while HT-DC users operate with water as secondary fluid. The saturated vapor CO_2 streams leaving C-4, C-5 and C-6 are mixed (stream 26) and superheated in the waste heat vaporizer H-2. Finally, the stream 27 is expanded in the turbine T2 to produce electricity.

Next, the LNG stream 4 still has an exergetic content valuable enough to be used in RC-3 as heat sink to condense CO_2 in C-3. Once pumped beyond its critical pressure by P4 and pre-heated in the recuperators R-2, the CO_2 stream 43 is heated in the biomass boiler H-3 and expanded in the high-pressure turbine T3 (HP). Stream 37 is re-heated and expanded again in the low-pressure turbine T3 (LP).

Finally, the LNG (stream 5) is completely regasified in the seawater heater H-4 and expanded to meet the pressure of the distribution pipeline and to produce extra electrical energy. If NG condenses at the exit of the LNG direct expansion unit (stream 7), an auxiliary seawater vaporizer (H-5) is activated to ensure that NG at gas phase is supplied to the end-users.

4.3. Plant modelling and performance parameters

The polygeneration plant was modelled and simulated with the software Engineering Equation Solver [63]. The following assumptions have been made:

- System operation under steady-state conditions.
- Thermal and pressure losses are neglected.
- The composition of natural gas is assumed as pure methane.
- Streams entering pumps P2, P3 and P4 (streams 12, 18 and 41, respectively) are at saturated liquid state.
- Streams of CO_2 leaving C-4, C-5 and C-6 (streams 21, 23 and 25, respectively) are at saturated vapor state.
- Streams of secondary refrigerants are at saturated vapor state at the inlet of C-4 and C-5 (streams 28 and 30) and at saturated liquid state at the exit (streams 29 and 31).
- Isentropic efficiencies of turbines and LNG expander: 85%.
- Isentropic efficiencies of pumps: 75%.
- Effectiveness of recuperators R-1 and R-2: 80%.

Heat transfer in the heat exchangers is calculated from energy balance equations ($\dot{Q} = \dot{m}_i\left(h_{i,in} - h_{i,out}\right) = \dot{m}_j\left(h_{j,out} - h_{j,in}\right)$) and temperatures, pressures and flow rates set in **Table 1**. The ε-NTU method is used to verify that the calculated values for inlet and outlet streams are feasible ($0 \leq \varepsilon \leq 1$). For the modelling of heat recuperators (R-1 and R-2), a constant heat transfer effectiveness is defined. In the case of the recuperator R-1 in power cycle RC-1, temperature differences between inlet/outlet streams are small and specific heat capacities can be treated as constant. Thus, the traditional definition of effectiveness is applied:

$$\varepsilon_{R-1} = \frac{\dot{Q}_{R-1}}{\dot{Q}_{max,R-1}} = \frac{\dot{Q}_{R-1}}{min(\dot{m}\cdot Cp)\cdot\Delta T_{max}} \cong \frac{T_{10}-T_{11}}{T_{10}-T_{13}} \quad (1)$$

Nevertheless, in the case of the recuperator R-2 in CO_2 transcritical power cycle RC-3, the temperature differences are higher and variations in specific heat must be considered. Thus, the definition of effectiveness given by Cayer et al. [64] has been used to model the recuperator R-2:

$$\varepsilon_{R-2} = \frac{\dot{Q}_{R-2}}{\dot{Q}_{max,R-2}} = \frac{\dot{Q}_{R-2}}{max\{\dot{m}_{39}[h_{39}-h_{40(T_{40}=T_{42})}];\ \dot{m}_{42}[h_{43(T_{43}=T_{39})}-h_{42}]\}} \quad (2)$$

The net power ($\dot{W}_{net} = \sum \dot{W}_T - \sum \dot{W}_P$) produced by each operational block is modelled as follows:

$$\dot{W}_{net,RC1} = \dot{W}_{T1} - \dot{W}_{P2} = \dot{m}_{RC1}[(h_9 - h_{10}) - (h_{13} - h_{12})] \quad (3)$$

$$\dot{W}_{net,RC2} = \dot{W}_{T2} - \dot{W}_{P3} = \dot{m}_{DC}[(h_{27} - h_{17}) - (h_{19} - h_{18})] \quad (4)$$

$$\dot{W}_{net,RC3} = \dot{W}_{T3HP} + \dot{W}_{T3LP} - \dot{W}_{P4} = \dot{m}_{RC3}[(h_{36} - h_{37}) + (h_{38} - h_{39}) - (h_{42} - h_{41})] \quad (5)$$

$$\dot{W}_{net,EXP} = \dot{W}_{EXP} - \dot{W}_{P1} = \dot{m}_{LNG}[(h_6 - h_7) - (h_2 - h_1)] \quad (6)$$

On the other hand, the cooling provided by the DC at each temperature level is:

$$\dot{Q}_{DC-LT} = \dot{m}_{20}(h_{21} - h_{20}) = \dot{m}_{28}(h_{28} - h_{29}) \quad (7)$$

$$\dot{Q}_{DC-MT} = \dot{m}_{22}(h_{23} - h_{22}) = \dot{m}_{30}(h_{30} - h_{31}) \quad (8)$$

$$\dot{Q}_{DC-HT} = \dot{m}_{24}(h_{24} - h_{25}) = \dot{m}_{32}(h_{32} - h_{33}) \quad (9)$$

Furthermore, an exergy analysis is performed to identify the inefficiencies of the processes in the plant and determinate how efficiently the LNG exergy is being exploited. The exergy content of each point is written as:

$$\dot{E}x_i = \dot{m}_i[(h_i - h_0) - T_0(s_i - s_0)] \quad (10)$$

Where the reference-environment (or dead state) temperature (T_0) and pressure (p_0) are set at 298 K and 101.3 kPa, respectively.

The exergy destroyed ($\dot{I} = \dot{E}x_{in} - \dot{E}x_{us} - \dot{E}x_{out}$) in each operating block of the plant is expressed as follows:

$$\dot{I}_{RC1} = \dot{E}x_2 - \dot{E}x_3 - \dot{W}_{net,RC1} - \left(\dot{E}x_{16} - \dot{E}x_{15}\right) \quad (11)$$

$$\dot{I}_{DC\&RC2} = \dot{E}x_3 - \dot{E}x_4 + \dot{E}x_{34} - \dot{E}x_{35} - \dot{W}_{net,RC2} - \left(\dot{E}x_{29} - \dot{E}x_{28}\right) - \left(\dot{E}x_{31} - \dot{E}x_{30}\right) - \left(\dot{E}x_{33} - \dot{E}x_{32}\right) \quad (12)$$

$$\dot{I}_{RC3} = \dot{Q}_{H-3}\left(1 - \frac{T_{bb}}{T_0}\right) + \dot{E}x_4 - \dot{E}x_5 - \dot{W}_{net,RC3} \quad (13)$$

$$\dot{I}_{EXP} = \left(\dot{E}x_5 + \dot{E}x_7\right) - \dot{W}_{net,EXP} - \left(\dot{E}x_{45} - \dot{E}x_{44}\right) \quad (14)$$

Finally, the exergetic efficiency ($\eta_{ex} = \dot{E}x_{us}/\dot{E}x_{in}$) of the whole polygeneration plant is defined as follows:

$$\eta_{ex,plant} = \frac{\sum \dot{W}_T + \dot{W}_{EXP} + (\dot{E}x_{29} - \dot{E}x_{28}) + (\dot{E}x_{31} - \dot{E}x_{30}) + (\dot{E}x_{33} - \dot{E}x_{32})}{(\dot{E}x_1 - \dot{E}x_8) + (\dot{E}x_{34} - \dot{E}x_{35}) + \dot{Q}_{H-3}\left(1 - \frac{T_{bb}}{T_0}\right) + \sum \dot{W}_P} \quad (15)$$

The exergetic efficiency given by Eq. (15) excludes the exergy content of regasified NG supplied to the distribution pipeline (point 8 in Fig. 7) as a useful exergy output of the plant. This is because we consider that the exergetic content at this point is not an indicator of the performance of the plant, but it depends only on the NG distribution pipeline requirements. However, as indicated in section 3.1, there is not a common agreement on a definition of the exergetic efficiency of the energy systems used for LNG cold recovery.

4.4. Performance indicators

To evaluate the performance of the polygeneration plant we define the following performance indicators:

- Total net power production of the plant ($\dot{W}_{net}$):

$$\dot{W}_{net,tot} = \dot{W}_{net,RC1} + \dot{W}_{net,RC2} + \dot{W}_{net,RC3} + \dot{W}_{net,EXP} \quad (16)$$

This parameter quantifies the net power produced by the power cycles RC-1, RC-2, RC-3 and the LNG direct expansion unit.

- District Cooling Service (DCS):

$$DCS = \dot{Q}_{DC,LT} + \dot{Q}_{DC,MT} + \dot{Q}_{DC,HT} \quad (17)$$

- Equivalent Electricity Saving (EES), measured in kWh/ton-LNG:

$$EES = \frac{1}{\dot{m}_{LNG}}\left(\dot{W}_{net,tot} + \frac{\dot{Q}_{DC,LT}}{EER_{ref,LT}} + \frac{\dot{Q}_{DC,MT}}{EER_{ref,MT}} + \frac{\dot{Q}_{DC,HT}}{EER_{ref,HT}}\right) \quad (18)$$

This indicator takes into account not only the electric power produced by the plant, but also the electrical energy saved by the district cooling network. Notice that, at present, the cold consumers need conventional refrigeration systems, so the use of LNG cold might suppose an electric energy saving. To estimate the electric energy saving by the district cooling network we transform the thermal energy to electrical energy by using a reference Energy Efficiency Ratio (EER_{ref}) for each temperature level. The EER_{ref} for the low, medium and high temperature district cooling are set to 1.3, 2.5, 4.0, respectively [65].

- Primary Energy Savings (PES):

$$PES = \frac{1}{\eta_{ref}}\left(\dot{W}_{net,tot} + \frac{\dot{Q}_{DC,LT}}{EER_{ref,LT}} + \frac{\dot{Q}_{DC,MT}}{EER_{ref,MT}} + \frac{\dot{Q}_{DC,HT}}{EER_{ref,HT}}\right) \quad (19)$$

This indicator evaluates the amount of primary energy saved by the polygeneration plant taking as a reference a typical thermal efficiency of a combined cycle power plant (η_{ref}=52%).

Furthermore, to evaluate the performance of the polygeneration plant from the environmental point of view, two indicators are defined:

- Seawater Saving (SWS):

$$SWS = \left(1 - \frac{\Sigma \dot{m}_{SW}}{\dot{m}_{SW,ref}}\right) \times 100\% \quad (20)$$

This indicator shows the reduction (in %) of seawater required by the proposed polygeneration plant with respect to the conventional LNG regasification process.

- Avoided CO_2 emissions (ACO_2e), measured in ton-CO_2/year:

$$ACO_2e = EF\left(\dot{W}_{net,tot} + \frac{\dot{Q}_{DC,LT}}{EER_{ref,LT}} + \frac{\dot{Q}_{DC,MT}}{EER_{ref,MT}} + \frac{\dot{Q}_{DC,HT}}{EER_{ref,HT}}\right) \quad (21)$$

where EF is the emission factor that is set to 0.308 kg-CO_2/kWh. This indicator aims to estimate the contribution of the polygeneration plant to reduce the CO_2 emissions. The final CO_2 equivalent emissions avoided could be even higher if the refrigerant leakages and other associated emissions of the replaced refrigeration plants were taken into account.

5. Results and discussion

The results obtained from the simulation of the polygeneration plant are presented as follows: First, the thermodynamic performance of the plant under different operating modes is analyzed. Second, the effect of the LNG pressure in the performance of the plant is investigated. And finally, an exergy analysis is conducted to evaluate how efficiently the LNG exergy is exploited by the plant. An operation base case is defined using the parameters listed in **Table 1**.

5.1. Performance analysis

The polygeneration plant proposed in this work is very flexible and can be operated in different operating modes. The studied operating modes are the following:

- Mode 0 (**RE**): Typical regasification process without LNG cold recovery.
- Mode 1 (**RE+EX**): LNG is regasified and electricity is produced in the LNG direct expansion unit EXP.
- Mode 2 (**RE+EX+PC**): LNG cold is exclusively used for electric power production. In this case, electricity is generated in the LNG direct expansion unit EXP and in power cycles RC-1 and RC-3. Modes 1 and 2 are the most used in the few plants worldwide that currently exploit LNG exergy.
- Mode 3 (**RE+DC**): LNG exergy is used only to provide cooling for the DC network. LNG is regasified without any electrical energy generation.
- Mode 4 (**CB**): This is a combined mode, so all operating blocks of the polygeneration plant work simultaneously. Therefore, LNG is regasified, the DC network is providing refrigeration service to "cold consumers" and electrical energy is produced.

Table 2 shows the performance results obtained for each operating mode listed above. The plant's subsystems that work in each mode are marked with an "X". The following conclusions can be drawn:

(a) Apart from the fact that LNG cold is not recovered in the typical regasification process (mode 0), an input of electrical energy is required (mainly by pumping). When the LNG direct expansion unit operates (mode 1) the electrical energy consumption of the plant decreases 53% and CO_2 emissions are reduced. However, the net power of the plant remains negative and the required amount of seawater is slightly higher. On the other hand, when the LNG cold is only used for electric power production (mode 2), the net power of the plant is 3.7 MW (31 kWh/ton-LNG). Moreover, the required amount of seawater is 24.5% lower than that required by the typical LNG regasification process.

(b) The refrigeration capacity is 12.5 MW (53.6 kWh/ton-LNG) when the LNG cold is used just for the DC network (mode 3). This amount of cold is distributed to the "cold consumers" as follows: 6.3 MW, 5.0 MW and 1.2 MW for LT-DC, MT-DC and HT-DC users, respectively. Under this operating mode the seawater saving is 54.8% respect to the typical LNG regasification and the saving of primary energy is 107 GWh/y. Because electrical energy is not produced in mode 3, the net power of the plant is negative. The reduction in CO_2 emissions is 73% greater than that of operating mode 2.

(c) The polygeneration plant exhibits the best performance when all its subsystems operate at once (mode 4), with an EES of 81.1 kWh/ton-LNG. The net power is 4.5 MW which is 21% higher than that of mode 2. Even though the refrigeration capacity decreases to 9 MW (28% lower than when operating under mode 3), the architecture of the plant allows switching to operating mode 3 for peaks in refrigeration demand. Under mode 4, the plant has an annual primary energy saving of 162 GWh. Regarding the environmental performance, the saving of seawater is 67.6% with respect to the typical LNG regasification and the emission of 35,284 ton-CO_2/y are avoided.

Table 3 breakdowns the contribution of each power cycle to the total net power produced by the polygeneration plant under operating mode 4. The power cycle RC-3 contributes most to the total net power mainly because it has the highest temperature heat source (biomass combustion). On the other hand, **Table 4** shows the amount of seawater required by each heat exchanger. Also, the ratio of seawater to the LNG mass flow rate is included. Notice that seawater heaters H-1 and H-4 accounts near 90% of the total seawater consumption of the plant, while H-5 is only used to ensure gas state of NG at the exit of the LNG direct expansion unit.

Table 5 offers a comparison between the equivalent electricity saving obtained by the polygeneration plant proposed in this work and the specific power obtained by most of the power cycles described in **section 3.1**. Although this comparison is quite weak because of the polygeneration plant simulated in this work is not a pure power generation plant, some basic conclusions can be obtained. On one hand, the specific power output of the plants that operates with BCs are much higher than that obtained by any other type of power cycle. Among other reasons because these cycles operate at higher temperatures. Thus, the polygeneration plant simulated is not comparable with these types of cycles. Nevertheless, the equivalent electricity saving of the plant is acceptable compared with the specific power output obtained by the rest of power cycles.

Table A1 in **Appendix A** shows the main thermophysical properties of each state point of the polygeneration plant given in **Fig. 7** when it operates under the combined mode (mode 4).

5.2. Effect of LNG pressure in the polygeneration plant

Figure 8 depicts the influence of the operating pressure of LNG in the performance of the plant. A range of pressures from 7 to 20 MPa is analyzed. The following observations can be made:

a) If the objective is to maximize the net power produced, the optimum pressure of LNG in the plant is 13.9 MPa. The net power given by the polygeneration plant operating at this pressure is 4.9 MW (**Fig. 8 (a)**), representing an increase of 8.2% compared to that obtained when the plant operates under the default pressure (8 MPa). Initially, the increase of pressure favors the mechanical power produced by the LNG direct expansion unit. However, for pressures higher than the optimal, this positive effect is offset by a reduction of the heat capacity of LNG and the net power produced decreases.

b) As shown in **Fig. 8 (a)**, the refrigeration capacity of the system decreases dramatically with LNG pressure. When the pressure of the plant is set to 13.9 MPa, the DCS decreases 17.7% with respect to the default scenario where the LNG pressure is set to 8 MPa. The main reason for this phenomenon is that the heat capacity rate of LNG decreases with pressure. On the other hand, **Figure 8 (b)** shows that the seawater consumption of the plant increases with the pressure. The seawater saved decreases 16.4% (with respect to the base case scenario) when the plant operates at 13.9 MPa. The EES indicator also decreases with the pressure, although to a minor extent.

c) **Figure 8 (c)** shows that the exergetic efficiency of the plant enhances with LNG pressure. The exergetic efficiency is 36.7% when the plant operates at 13.9 MPa, which is slightly higher than when operating at 8 MPa (34.7%). This behavior is due mainly to the lower exergy input from waste heat and the higher power production by the LNG direct expansion unit that both counteract the higher power consumption of pump P1 and the lower DC service when LNG pressure increases. On the other hand, as shown in **Fig. 8 (d)**, both the primary energy saving and the reduction in CO_2 emissions decrease with LNG pressure.

d) Although the net power increases when the pressure is above 8 MPa (<13.9 MPa), the rest of indicators get worse. In the case of the exergetic efficiency, the increasing is too low to justify working at high LNG pressures. In fact, in percentage terms, the increasing in the net power produced and in the exergetic efficiency are lower than the decreasing of the rest of indicators, especially the cooling capacity. Therefore, we determined that the operating pressure of the plant should be kept at to the minimum possible value (8 MPa) to guarantee the DC service to the "cold consumers". Nonetheless, the pressure of the plant reveals to be a key control variable. Hence, the pressure of the plant will remain at its minimum value (8 MPa) when the refrigeration demand is maximum, while this pressure may be increased to produce more electricity when refrigeration demand decreases.

Fig. 8. Variation of (a) the net power and DCS, (b) the EES and SWS, (c) the exergetic efficiency and the exergy input from waste heat and (d) the PES and ACO_2e with the LNG pressure in the polygeneration plant.

5.3. Exergetic analysis

An exergetic analysis was required to fully analyze the system performance. **Table 2** shows the exergetic efficiencies of each operating scenario. The combined operating mode (mode 4) exhibits the best exergetic efficiency (34.7%), which is quite higher than that of the rest of operating modes.

Figure 9 illustrates the exergy flow diagram of LNG from the inlet when it leaves the pump P1 to the final outlet of regasified NG supplied to the distribution pipeline. The LNG exergy exploited by the polygeneration plant is 41.5% (13.5 MW) of the total LNG exergy content (32.6 MW) at the exit of pump P1. Of this quantity, the DC network and the power cycle RC-2 exploits almost a half of it. Power cycles RC-1 and RC-3 exploits 11.5% and 6.9% of LNG exergy, respectively. Notice that the regasified NG retains 58.5% of the LNG exergy at the exit of pump P1.

Fig. 9. LNG exergy flow diagram for the polygeneration plant. Percentages are based on the LNG exergy at the exit of the pump P1.

Table 6 shows the exergy destroyed in each unit. The subsystem with the highest exergy destruction is the power cycle RC-3, mainly due to the irreversibility of the biomass boiler. On the other hand, the total exergy destroyed in the condensers where LNG is used as heat sink (C-1, C-2 and C-3) contributes with the largest portion of exergy destroyed in the plant (43.7%). In particular, the condenser C-2 of the DC network and power cycle RC-2 accounts near a quarter of the total exergy destroyed. The exergy destroyed by the seawater heaters accounts 11% and the contribution of pumps to the total irreversibility is only 6%.

6. Conclusions

In this paper, the LNG supply chain and the conventional regasification technologies were analyzed to identify the cold recovery opportunities. Also, the barriers that currently block LNG cold recovery were highlighted. On the other hand, the main existing applications and technologies for LNG cold recovery were overviewed. Although there many applications and technologies for this purpose, most of them are immatures and their implementation is not widespread. Besides, most of the literature is focused on exploiting LNG cold for a single application, while LNG cold offers a lot of possibilities of exploitation via polygeneration. As a case study, we proposed and modelled a polygeneration plant for power and cold production where cold from LNG-regasification is recovered. The main conclusions are:

- The polygeneration plant is an example of the integration of a LNG cold recovery system in a regasification facility which has a potential cold consumer nearby. The LNG exergy is exploited in cascade to produce electrical power and to give district cooling service at three levels of temperature for a wide type of cold consumers. Furthermore, the plant operates exclusively with natural fluids with nearly no environmental impact.

- The flexibility of the plant enables to operate in different modes. The production of net power and cooling is 4.5 MW and 9 MW, respectively when all the subsystems of the plant work simultaneously and for a LNG regasification capacity of 29.9 kg s^{-1}. In this case, the equivalent electricity saving of the plant is 81.1 kWh/ton-LNG. Regarding the environmental impact, the plant contributes to reduce 67.6% the seawater consumed by the typical LNG regasification process and it avoids the annual emission of 35,284 ton-CO_2.

- The effect of the operating LNG pressure in the performance of the plant is remarkable. While in general a rise of LNG pressure supposes an increase of the net power produced, the district cooling service decreases strongly. Thus, the LNG pressure is an important control variable of the system; pressure can be the minimum when the refrigeration demand is high while it can be raised to produce extra electrical power when the refrigeration demand decreases.

- The exergy analysis reveals that 34.7% of the total exergy used by the plant is being converted into useful work. Therefore, there is room for improvement and further upgrades may be applied to boost the performance of the plant.

Acknowledgements

Antonio Atienza-Márquez acknowledges the Spanish Ministry of Education the financial support of the predoctoral contract FPU15/04514. The authors also thank Mr Nasiruddin T Sheikh for providing helpful information.

Appendix. A

Table A1. Thermophysical properties of each state point of the polygeneration plant

References

[1] IEA, CO2 Emissions from Fuel Combustion 2017, OECD Publishing, Paris, 2017. doi:10.1787/co2_fuel-2017-en.

[2] S. Kumar, H.T. Kwon, K.H. Choi, W. Lim, J.H. Cho, K. Tak, I. Moon, LNG: An eco-friendly cryogenic fuel for sustainable development, Appl. Energy. 88 (2011) 4264–4273. doi:10.1016/j.apenergy.2011.06.035.

[3] W. Mazyan, A. Ahmadi, H. Ahmed, M. Hoorfar, Market and technology assessment of natural gas processing: A review, J. Nat. Gas Sci. Eng. 30 (2016) 487–514. doi:10.1016/j.jngse.2016.02.010.

[4] IEA, Key World Energy Statistics, Paris, 2017. doi:10.1787/key_energ_stat-2017-en.

[5] BP Energy Outlook - 2017 edition, (2017) 1–103. https://www.bp.com/content/dam/bp/pdf/energy-economics/energy-outlook-2017/bp-energy-outlook-2017.pdf (accessed September 13, 2017).

[6] DNV GL, Oil and Gas Forecast to 2050. Energy Transition Outlook 2017, (2017) 76.

[7] H.-M. Chang, A thermodynamic review of cryogenic refrigeration cycles for liquefaction of natural gas, Cryogenics (Guildf). 72 (2015) 127–147. doi:10.1016/j.cryogenics.2015.10.003.

[8] International Gas Union (IGU), IGU World LNG Report - 2017 Edition, 2017.

[9] T. Sung, K.C. Kim, LNG Cold Energy Utilization Technology, in: Energy Solut. to

Combat Glob. Warm. Lect. Notes Energy 33, Springer, Cham, 2017: pp. 47–66. doi:10.1007/978-3-319-26950-4_3.

[10] CORE LNGas hive, (2016). www.corelngashive.eu (accessed June 26, 2017).

[11] HDGAS - Horizon 2020, (2017). http://www.hdgas.eu/ (accessed September 7, 2017).

[12] CryoHub - Cryogenic Energy Storage for Renewable Refrigeration and Power Supply, (2017). http://cryohub.eu/en-gb/ (accessed September 7, 2017).

[13] O. Koku, S. Perry, J.K. Kim, Techno-economic evaluation for the heat integration of vaporisation cold energy in natural gas processing, Appl. Energy. 114 (2014) 250–261. doi:10.1016/j.apenergy.2013.09.066.

[14] M. Mehrpooya, M. Omidi, A. Vatani, Novel mixed fluid cascade natural gas liquefaction process configuration using absorption refrigeration system, Appl. Therm. Eng. 98 (2016) 591–604. doi:10.1016/j.applthermaleng.2015.12.032.

[15] M.S. Khan, I.A. Karimi, D.A. Wood, Retrospective and future perspective of natural gas liquefaction and optimization technologies contributing to efficient LNG supply: A review, J. Nat. Gas Sci. Eng. 45 (2017) 165–188. doi:10.1016/j.jngse.2017.04.035.

[16] Qatargas - Future Fleet, (2014). http://www.qatargas.com/English/AboutUs/Pages/FutureFleet.aspx (accessed September 7, 2017).

[17] Enagas, Barcelona Regasification Plant, (2014). http://www.enagas.es/enagas/en/Transporte_de_gas/PlantasRegasificacion/PlantaBarcelona (accessed September 7, 2017).

[18] E. Querol, B. Gonzalez-Regueral, J. García-Torrent, M.J. García-Martínez, Boil off gas (BOG) management in Spanish liquid natural gas (LNG) terminals, Appl. Energy. 87 (2010) 3384–3392. doi:10.1016/j.apenergy.2010.04.021.

[19] B.B. Kanbur, L. Xiang, S. Dubey, F.H. Choo, F. Duan, Cold utilization systems of LNG: A review, Renew. Sustain. Energy Rev. 79 (2017) 1171–1188. doi:10.1016/j.rser.2017.05.161.

[20] Z. Deng, K. Hui, Y. Zhang, Y. Cao, Numerical simulation analysis of the flow field and convective heat transfer in new super open rack vaporizer, Appl. Therm. Eng. 106 (2016) 721–730. doi:10.1016/j.applthermaleng.2016.03.071.

[21] T. Morosuk, G. Tsatsaronis, LNG - Based Cogeneration Systems: Evaluation Using Exergy-Based Analyses, in: Nat. Gas - Extr. to End Use, 2012. http://dx.doi.org/10.5772/51477 (accessed September 22, 2017).

[22] S. Mokhatab, J.Y. Mak, J. V Valappil, D.A. Wood, Handbook of Liquefied Natural Gas, Elsevier Science, 2013. https://books.google.es/books?id=nQswAAAAQBAJ.

[23] A. Bath, B. Shackleton, C. Botica, Development of temperature criteria for marine discharge from a large industrial seawater supplies project in Western Australia, Water SA. 30 (2004) 648–654.

[24] L. Pu, Z. Qu, Y. Bai, D. Qi, K. Song, P. Yi, Thermal performance analysis of intermediate fluid vaporizer for liquefied natural gas, Appl. Therm. Eng. 65 (2014) 564–574. doi:10.1016/j.applthermaleng.2014.01.031.

[25] S. Xu, Q. Cheng, L. Zhuang, B. Tang, Q. Ren, X. Zhang, LNG vaporizers using various refrigerants as intermediate fluid: Comparison of the required heat transfer area, J. Nat. Gas Sci. Eng. 25 (2015) 1–9. doi:10.1016/j.jngse.2015.04.031.

[26] D. Pineda Quijano, C. Infante Ferreira, W. Duivenvoorden, J. Mieog, T. Van Der Noortgaete, B. Van Der Velpen, Techno-economic feasibility study of a system for the transfer of refrigeration capacity from LNG regasification plants to industrial assets, in: 12th IEA Heat Pump Conf., Rotterdam, 2017.

[27] C. Qi, W. Wang, B. Wang, Y. Kuang, J. Xu, Performance analysis of submerged combustion vaporizer, J. Nat. Gas Sci. Eng. 31 (2016) 313–319. doi:10.1016/j.jngse.2016.03.003.

[28] Y.C. Park, J. Kim, Submerged combustion vaporizer optimization using Entropy Minimization Method, Appl. Therm. Eng. 103 (2016) 1071–1076. doi:10.1016/j.applthermaleng.2016.04.133.

[29] International Institute of Refrigeration, Liquefied Natural Gas: Current Expansion and Perspectives. 19-th Informatory Note on Refrigerating Technologies, Paris (France), 2006. http://www.iifiir.org/userfiles/file/publications/notes/NoteTech_19_EN.pdf (accessed September 22, 2017).

[30] United Nations - Framework Convention on Climate Change, The Paris Agreement, (2015). http://unfccc.int/paris_agreement/items/9485.php (accessed September 17, 2017).

[31] European Comision, An EU Strategy on Heating and Cooling, (2016) 13. ec.europa.eu/energy/sites/ener/files/documents/1_EN_ACT_part1_v14.pdf (accessed September 20, 2017).

[32] A. An Mota-Babiloni, J. Navarro-Esbrí, A. Barrag An-Cervera, F. Mol Es, B. Peris, Analysis based on EU Regulation No 517/2014 of new HFC/HFO mixtures as alternatives of high GWP refrigerants in refrigeration and HVAC systems, Int. J. Refrig. 52 (2015) 21–31. doi:10.1016/j.ijrefrig.2014.12.021.

[33] S. Hirakawa, K. Kosugi, Utilization of LNG cold, Int. J. Refrig. 4 (1981) 17–21. doi:10.1016/0140-7007(81)90076-1.

[34] H. Uwitonze, S. Han, C. Jangryeok, K.S. Hwang, Design process of LNG heavy hydrocarbons fractionation: Low LNG temperature recovery, Chem. Eng. Process. Process Intensif. 85 (2014) 187–195. doi:10.1016/j.cep.2014.09.002.

[35] Y. Li, H. Luo, Integration of light hydrocarbons cryogenic separation process in refinery based on LNG cold energy utilization, Chem. Eng. Res. Des. 93 (2015) 632–639. doi:10.1016/j.cherd.2014.04.009.

[36] I. Lee, J. Park, I. Moon, Conceptual Design and Exergy Analysis of Combined Cryogenic Energy Storage and LNG Regasification Processes: Cold and Power Integration, Energy. (2017). doi:10.1016/j.energy.2017.08.054.

[37] M. Romero Gómez, R. Ferreiro Garcia, J. Romero Gómez, J. Carbia Carril, Review of thermal cycles exploiting the exergy of liquefied natural gas in the regasification process, Renew. Sustain. Energy Rev. 38 (2014) 781–795. doi:10.1016/j.rser.2014.07.029.

[38] P.A. Ferreira, I. Catarino, D. Vaz, Thermodynamic analysis for working fluids comparison in Rankine-type cycles exploiting the cryogenic exergy in Liquefied Natural Gas (LNG) regasification, Appl. Therm. Eng. 121 (2017) 887–896. doi:10.1016/j.applthermaleng.2017.04.082.

[39] M.H. Ahmadi, M. Mehrpooya, F. Pourfayaz, Thermodynamic and exergy analysis and optimization of a transcritical CO2 power cycle driven by geothermal energy with liquefied natural gas as its heat sink, Appl. Therm. Eng. 109 (2016) 640–652. doi:10.1016/j.applthermaleng.2016.08.141.

[40] K.H. Kim, K.C. Kim, Thermodynamic performance analysis of a combined power cycle using low grade heat source and LNG cold energy, Appl. Therm. Eng. 70 (2014) 50–60. doi:10.1016/j.applthermaleng.2014.04.064.

[41] G. Oliveti, N. Arcuri, R. Bruno, M. De Simone, A rational thermodynamic use of liquefied natural gas in a waste incinerator plant, Appl. Therm. Eng. 35 (2012) 134–144. doi:10.1016/j.applthermaleng.2011.10.015.

[42] R. Ferreiro García, J. Jose, Carbia Carril, J. Romero Gómez, M. Romero Gómez, Combined cascaded Rankine and direct expander based power units using LNG (liquefied natural gas) cold as heat sink in LNG regasification, Energy. 105 (2016) 16–24. doi:10.1016/j.energy.2015.09.051.

[43] X. Shi, B. Agnew, D. Che, J. Gao, Performance enhancement of conventional combined cycle power plant by inlet air cooling, inter-cooling and LNG cold energy utilization, Appl. Therm. Eng. 30 (2010) 2003–2010. doi:10.1016/j.applthermaleng.2010.05.005.

[44] K. Kaneko, K. Ohtani, Y. Tsujikawa, S. Fujii, Utilization of the cryogenic exergy of LNG by a mirror gas-turbine, Appl. Energy. 79 (2004) 355–369. doi:10.1016/j.apenergy.2004.02.007.

[45] C. Dispenza, G. Dispenza, V. La Rocca, G. Panno, Exergy recovery during LNG regasification: Electric energy production - Part one, Appl. Therm. Eng. 29 (2009) 380–387. doi:10.1016/j.applthermaleng.2008.03.036.

[46] C. Dispenza, G. Dispenza, V. La Rocca, G. Panno, Exergy recovery during LNG regasification: Electric energy production – Part two, Appl. Therm. Eng. 29 (2009) 388–399. doi:10.1016/j.applthermaleng.2008.03.035.

[47] T. Morosuk, G. Tsatsaronis, Comparative evaluation of LNG – based cogeneration systems using advanced exergetic analysis, Energy. 36 (2011) 3771–3778. doi:10.1016/j.energy.2010.07.035.

[48] M. Romero Gómez, R.F. Garcia, J.C. Carril, J. Romero Gómez, High efficiency power plant with liquefied natural gas cold energy utilization, J. Energy Inst. 87 (2014) 59–68. doi:10.1016/j.joei.2014.02.007.

[49] T. Lu, K.S. Wang, Analysis and optimization of a cascading power cycle with liquefied natural gas (LNG) cold energy recovery, Appl. Therm. Eng. 29 (2009) 1478–1484. doi:10.1016/j.applthermaleng.2008.06.028.

[50] T. Miyazaki, Y.. Kang, A. Akisawa, T. Kashiwagi, A combined power cycle using refuse incineration and LNG cold energy, Energy. 25 (2000) 639–655. doi:10.1016/S0360-5442(00)00002-5.

[51] K. Wang, S. Dubey, F.H. Choo, F. Duan, Thermoacoustic Stirling power generation from LNG cold energy and low-temperature waste heat, Energy. 127 (2017) 280–290. doi:10.1016/j.energy.2017.03.124.

[52] M. Mehrpooya, M. Kalhorzadeh, M. Chahartaghi, Investigation of novel integrated air separation processes, cold energy recovery of liquefied natural gas and carbon dioxide power cycle, J. Clean. Prod. 113 (2016) 411–425. doi:10.1016/j.jclepro.2015.12.058.

[53] A. Ebrahimi, M. Ziabasharhagh, Optimal design and integration of a cryogenic Air Separation Unit (ASU) with Liquefied Natural Gas (LNG) as heat sink, thermodynamic and economic analyses, Energy. 126 (2017) 868–885. doi:10.1016/j.energy.2017.02.145.

[54] M. Mehrpooya, R. Esfilar, S.M.A. Moosavian, Introducing a novel air separation process based on cold energy recovery of LNG integrated with coal gasification, transcritical carbon dioxide power cycle and cryogenic CO 2 capture, J. Clean. Prod. 142 (2017) 1749–1764. doi:10.1016/j.jclepro.2016.11.112.

[55] W. Cao, C. Beggs, I.M. Mujtaba, Theoretical approach of freeze seawater desalination on flake ice maker utilizing LNG cold energy, Desalination. 355 (2014) 22–32. doi:10.1016/j.desal.2014.09.034.

[56] W. Lin, M. Huang, A. Gu, A seawater freeze desalination prototype system utilizing LNG cold energy, Int. J. Hydrogen Energy. 42 (2017) 18691–18698. doi:10.1016/j.ijhydene.2017.04.176.

[57] C. Xie, L. Zhang, Y. Liu, Q. Lv, G. Ruan, S.S. Hosseini, A direct contact type ice generator for seawater freezing desalination using LNG cold energy, Desalination. (2017) 0–1. doi:10.1016/j.desal.2017.04.002.

[58] V. La Rocca, Cold recovery during regasification of LNG part one: Cold utilization far from the regasification facility, Energy. 35 (2010) 2049–2058. doi:10.1016/j.energy.2010.01.022.

[59] V. La Rocca, Cold recovery during regasification of LNG part two: Applications in an Agro Food Industry and a Hypermarket, Energy. 36 (2011) 4897–4908. doi:10.1016/j.energy.2011.05.034.

[60] C. Dispenza, G. Dispenza, V. La Rocca, G. Panno, Exergy recovery in regasification facilities - Cold utilization: A modular unit, Appl. Therm. Eng. 29 (2009) 3595–3608. doi:10.1016/j.applthermaleng.2009.06.016.

[61] A. Messineo, G. Panno, LNG cold energy use in agro-food industry: A case study in Sicily, J. Nat. Gas Sci. Eng. 3 (2011) 356–363. doi:10.1016/j.jngse.2011.02.002.

[62] Enagás, Barcelona Regasification Plant, (2014). http://www.enagás.nom.es/stfls/EnagasImport/Ficheros/684/890/Ficha Planta BARCELONA -19febrero2014- web ENG.pdf (accessed October 7, 2017).

[63] F-Chart Software, Engineering Equation Solver (EES), (2017). http://www.fchart.com/ees/ (Accesed 02.10.2017).

[64] E. Cayer, N. Galanis, M. Desilets, H. Nesreddine, P. Roy, Analysis of a carbon dioxide transcritical power cycle using a low temperature source, Appl. Energy. 86 (2009) 1055–1063. doi:10.1016/j.apenergy.2008.09.018.

[65] ASHRAE, ASHRAE Handbook-Refrigeration - SI Edition, 2014.

Nomenclature

Abbreviatures

1, 2, … ,47	Thermodynamic state points
ASU	Air separation unit
BB	Biomass boiler
BC	Brayton cycle
C-1…C-6	Condensers
DC	District Cooling
DCS	District Cooling service
EES	Equivalent Electricity Saving
EXP	LNG direct expander
FD	Freeze desalination
H-1…H-5	Heaters
HT	High-temperature (District Cooling)
IFV	Intermediate fluid vaporizer
LNG	Liquefied Natural Gas
LT	Low-temperature (District Cooling)
MT	Medium-temperature (District Cooling)
MTPA	Million tons per annum
NG	Natural Gas

ORV	Open rack vaporizer
P1…P4	Pumps
PES	Primary energy saving
R-1, R-2	Recuperators
RC	Rankine cycle
SCV	Submerged combustion vaporizer
SWS	Seawater Saving
T1…T4	Turbines

Variables

Cp	Specific heat (kJ kg^{-1} K^{-1})
$\dot{E}x$	Exergy (kW)
h	Enthalpy (kJ kg^{-1})
$\dot{I}$	Irreversibility (kW)
$\dot{m}$	Mass flow rate (kg s^{-1})
p	Pressure (Pa)
Q	Heat flux (kW)
s	Entropy (kJ kg^{-1} K^{-1})
T	Temperature (K)
$\dot{W}$	Power (kW)

Greek letters

Δ	Temperature difference (K)
ε	Effectiveness
η	Efficiency (%)

Subscripts

0	Reference environment (exergy)
bb	Biomass boiler
ex	Exergetic
net	Net (power)
sw	Seawater

Table 1. Base case operation parameters.

Block	Parameter	Value
LNG	LNG mass flow rate, ($\dot{m}_{LNG}$)	29.9 kg s^{-1}
	LNG storage pressure, (p_1)	0.13 MPa
	LNG storage temperature, (T_1)	-162°C
	Operating pressure of LNG in the plant	8 MPa
RC-1	High pressure RC-1	16.95 MPa
	Condensing temperature RC-1	-127.5°C
	ΔT between streams leaving C-1 ($T_{12} - T_3$)	5°C
	Inlet temperature of turbine T1, (T_9)	10°C
	Seawater inlet/outlet temperature H-1	20/15°C
DC+RC-2	DC share of refrigeration demand LT/MT/HT	50/40/10%
	DC supply pressure (main pipeline)	1.45 MPa
	DC supply temperature (main pipeline)	-50°C
	ΔT between streams leaving C-2 ($T_{18} - T_4$)	15°C
	Secondary fluid supply/return temperature HT-DC	5/12°C
	Secondary refrigerant supply temperatures LT/MT	-25/-10°C
	Inlet temperature of turbine T2, (T_{27})	30°C
	Waste heat (water) stream inlet/outlet temperature	40/35°C
RC-3	Combustion temperature inside biomass boiler, (T_{bb})	850°C
	Condensing temperature RC-3	5°C
	Heat output of biomass boiler	10 MW
	Inlet temperature of T4 (HP) and T4 (LP), (T_{36}, T_{38})	400°C
	High pressure RC-3	25 MPa
	Intermediate pressure RC-3	13.1 MPa
EXP	Inlet temperature of EXP, (T_6)	5°C
	Seawater inlet/outlet temperature H-4, H-5	20/15°C
	Temp. of NG supplied to distribution pipeline, (T_8)	5°C
	Pressure of NG supplied to distribution pipeline, (p_8)	7 MPa

Table 2. Performance indicators of the polygeneration plant for different operating modes.

Operation modes						Indicators						
Mode	**D**	**RC**	**RC**	**RC**	**T**	$\dot{W}_{net}$	**DCS**	**EES,**	**PES** [a],	**SWS**	**ACO_2**	$\eta_{ex,plant}$

	C	-1	-2	-3	E	, MW	, MW	kWh/ton-LNG	GWh/y	, %	e [b], ton-CO_2/y	, %
0: RE						-0.74	0	-6.2	-12.4	0	+2,706	0
1: R+EX					X	-0.34	0	-2.9	-5.7	-1.8	+1,241	2.9
2: RE+EX+PC		X		X	X	3.7	0	31.0	62.0	24.5	-13,512	24.5
3: RE+DC	X					-0.74	12.5	53.6	107.2	54.8	-23,348	14.2
4: CB	X	X	X	X	X	4.5	9.0	81.1	162.0	67.6	-35,284	34.7

[a] Taking as a reference an efficiency of 52%.

[b] Considering an emission factor of 0.308 kg-CO_2/kWh.

Table 3. Contribution of the power cycles of the plant to the total net power produced when operating under the combined mode (mode 4: CB).

Power cycle	$\sum \dot{W}_T$, MW	$\sum \dot{W}_P$, MW	$\dot{W}_{net}$, MW
RC-1	1.3	0.50	0.8
RC-2	0.82	0.023	0.8
RC-3	3.9	0.66	3.2
EXP	0.40	0.74	-0.34
Total	6.5	1.9	4.5

Table 4. Seawater consumed by the plant operating under the combined mode (mode 4: CB).

Subsystem	H-1	H-4	H-5	Total
$\dot{m}_{SW}$, kg s^{-1}	163.7	152.1	36.9	352.7
$\dot{m}_{SW}/\dot{m}_{LNG}$, (-)	5.47	5.09	1.23	11.79
$\dot{m}_{SW}/\dot{m}_{SW,tot}$, %	46.4	43.1	10.5	100

Table 5. Comparison of the equivalent energy saving of the polygeneration plant presented in this work with the specific power obtained by some power cycles studied in the literature.

Reference	Type of cycle	Working fluids	Top temperature	Plant output, kWh/ton-LNG
Ferreira et al. [38]	RC	Propene	16°C (seawater)	13.6
Ahmadi et al. [39]	Transcritical RC	CO_2	140°C (geothermal)	44
Oliveti et al. [41]	Two RCs + LNG direct expansion	Steam and ammonia	400°C (steam)	79.6
Ferreiro García et al. [42]	Two RCs + LNG direct expansion	Argon and methane	15°C (seawater)	65.3
Dispenza et al. [46]	Open BC + closed BC	Flue gas and He	579°C (helium)	380
Morosuk and Tsaronis [47]	Open BC + closed BC	Flue gas and N_2	1290°C (flue gas), 435°C (N_2)	531
Romero Gómez et al. [48]	Closed BC + RC	He (BC) and CO_2 (RC)	1300°C (combustion heat)	684.7
Lu and Wang [49]	Open BC + RC+ LNG direct exp.	Flue gas (BC) and ammonia-water (RC)	993.2°C (combustion gas)	139
Miyazaki et al. [50]	RC + LNG direct expansion	Ammonia-water (RC)	950°C (combustion gas)	105
This work	Three RCs and DC network	Argon and CO_2	400°C (CO_2)	81.1

Table 6. Irreversibility values for the components of the polygeneration plant.

Subsystem	Equipment	$\dot{I}$, kW	$\dot{I}$, %
RC-1	Condenser C-1	891.8	6.1%
	Pump P2	226.3	1.6%
	Recuperator R-1	5.4	0.0%
	SW heater H-1	1236.0	8.5%
	Turbine T1	386.0	2.6%
	Subtotal	2745.5	18.8%
DC & RC-2	Condenser C-2	3497.0	24.0%
	Pump P3	7.8	0.1%
	Condenser C-4	128.9	0.9%
	Condenser C-5	350.0	2.4%
	Condenser C-6	154.4	1.1%
	Vaporizer H-2	219.7	1.5%
	Turbine T2	169.1	1.2%
	Subtotal	4526.9	31.1%
RC-3	Condenser C-3	1983.0	13.6%
	Pump P4	166.0	1.1%
	Recuperator R-2	907.5	6.2%
	Biomass boiler H-3	2907.0	19.9%
	Turbine T3 (HP)	125.2	0.9%
	Turbine T3 (LP)	240.0	1.6%
	Subtotal	6328.7	43.4%

LNG EXP	Pump P1	481.9	3.3%
	SW vaporizer H-4	368.8	2.5%
	Expander EXP	78.1	0.5%
	SW vaporizer H-5	49.1	0.3%
	Subtotal	977.8	6.7%
	Total	14578.9	100.0%

Table A1. Thermophysical properties of each state point of the polygeneration plant

Nº	Fluid	$\dot{m}$ (kg s^{-1})	T (^{o}C)	p (MPa)	h (kJ kg^{-1})	s (kJ kg^{-1} K^{-1})	$\dot{E}x$ (kW)	Nº	Fluid	$\dot{m}$ (kg s^{-1})	T (^{o}C)	p (MPa)	h (kJ kg^{-1})	S (kJ kg^{-1} K^{-1})	$\dot{E}x$ (kW)
1	LNG	29.9	-162	0.13	-912.7	-6.693	32350	25	CO_2	2.6	-29.5	1.45	-69.92	-0.7433	398.9
2	LNG	29.9	-158.2	8.0	-888	-6.639	32606	26	CO_2	26.3	-29.5	1.45	-69.92	-0.7433	3989
3	LNG	29.9	-132.5	8.0	-798.5	-5.937	29024	27	CO_2	26.3	30	1.45	-9.493	-0.5207	3834
4	LNG	29.9	-65	8.0	-470.8	-4.085	22326	28	NH_3	3.4	-25	0.1515	1431	5.983	229.4
5	LNG	29.9	-27.2	8.0	-245.7	-3.077	20074	29	NH_3	3.4	-25	0.1515	86.12	0.5645	1134
6	LNG	29.9	5	8.0	-139.4	-2.67	19624	30	NH_3	2.8	-10	0.2908	1451	5.757	433.2
7	LNG	29.9	-3.9	7.0	-152.7	-2.661	19147	31	NH_3	2.8	-10	0.2908	154	0.8291	910.4
8	LNG	29.9	5	7.0	-126.9	-2.567	19079	32	Water	30.7	12	0.2	50.55	0.1804	39.7
9	Ar	26.5	10	16.95	-39.9	-1.183	8303	33	Water	30.7	5	0.2	21.22	0.07625	92.06
10	Ar	26.5	-98	3.998	-86.94	-1.134	6668	34	Water	75.9	40	0.1013	167.6	0.5722	118.3
11	Ar	26.5	-103.8	3.998	-92.2	-1.165	6771	35	Water	75.9	35	0.1013	146.7	0.5049	53.66
12	Ar	26.5	-127.5	3.998	-193	-1.843	9460	36	CO_2	21.9	400	25.0	337.7	-0.297	9336
13	Ar	26.5	-105.3	16.95	-174.2	-1.815	9734	37	CO_2	21.9	331.9	13.1	272.5	-0.2778	7782
14	Ar	26.5	-101.8	16.95	-168.9	-1.783	9626	38	CO_2	21.9	400	13.1	353	-0.1516	8723
15	Water	163.7	20	0.1013	83.93	0.2962	27.33	39	CO_2	21.9	284.8	3.969	238.7	-0.1148	5979
16	Water	163.7	15	0.1013	63.01	0.2242	114	40	CO_2	21.9	73.8	3.969	13.12	-0.6227	4355
17	CO_2	26.3	-13.6	0.6823	-40.88	-0.4991	2841	41	CO_2	21.9	5	3.969	-294.3	-1.696	4625
18	CO_2	26.3	-50	0.6823	-413.9	-2.16	6042	42	CO_2	21.9	25.2	25.0	-264.1	-1.67	5119
19	CO_2	26.3	-49.7	1.45	-413	-2.159	6057	43	CO_2	21.9	130.8	25.0	-38.55	-1.023	5836
20	CO_2	13.1	-49.7	1.45	-413	-2.159	3029	44	Water	152.1	20	0.1013	83.93	0.2962	25.38
21	CO_2	13.1	-29.5	1.45	-69.92	-0.7433	1995	45	Water	152.1	15	0.1013	63.01	0.2242	105.9
22	CO_2	10.5	-49.7	1.45	-413	-2.159	2423	46	Water	36.9	20	0.1013	83.93	0.2962	6.158
23	CO_2	10.5	-29.5	1.45	-69.92	-0.7433	1596	47	Water	36.9	15	0.1013	63.01	0.2242	25.69
24	CO_2	2.6	-49.7	1.45	-413	-2.159	605.7								

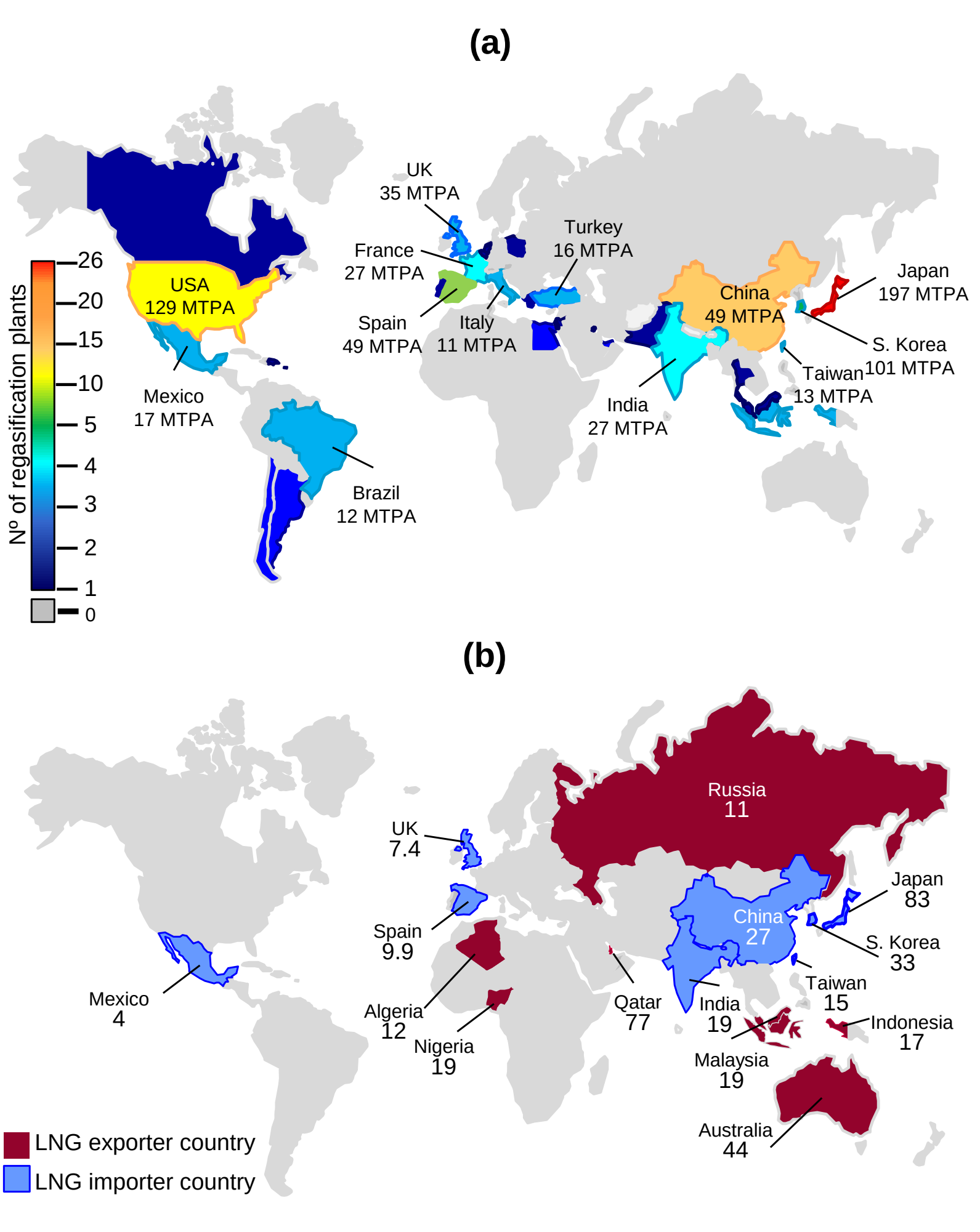
(a)
Nº of regasification plants
26
20
15
10
5
4
3
2
1
0
USA
129 MTPA
Mexico
17 MTPA
Brazil
12 MTPA
UK
35 MTPA
France
27 MTPA
Spain
49 MTPA
Italy
11 MTPA
Turkey
16 MTPA
China
49 MTPA
India
27 MTPA
Japan
197 MTPA
S. Korea
101 MTPA
Taiwan
13 MTPA
(b)
Russia
11
UK
7.4
Spain
9.9
Algeria
12
Nigeria
19
Mexico
4
Qatar
77
China
27
India
19
Malaysia
19
Japan
83
S. Korea
33
Taiwan
15
Indonesia
17
Australia
44
LNG exporter country
LNG importer country

$\eta_{Carnot} = 62.1\%$

$T_H - T_C = 182\ K$

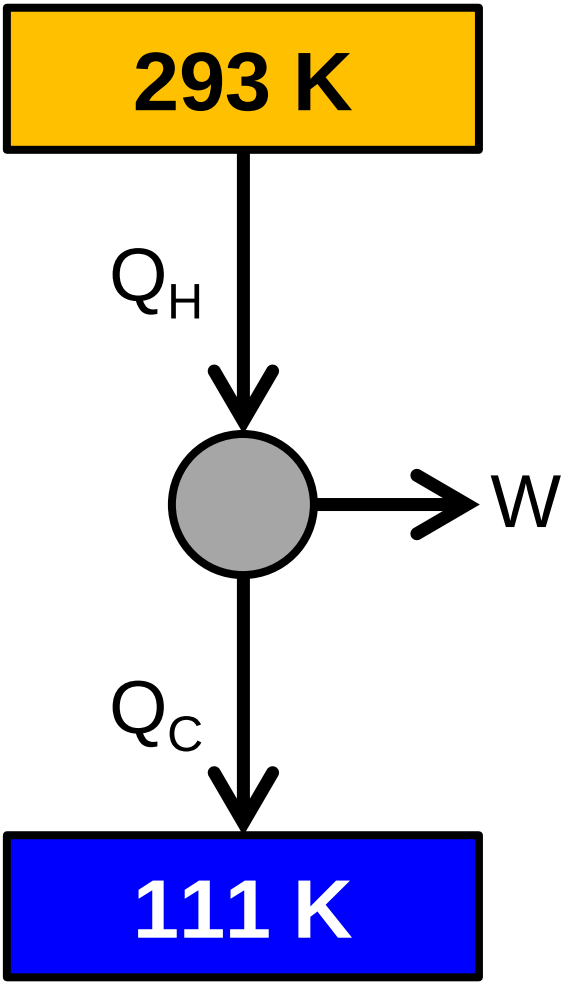

$\eta_{Carnot} = 62.1\%$

$T_H - T_C = 480.3\ K$

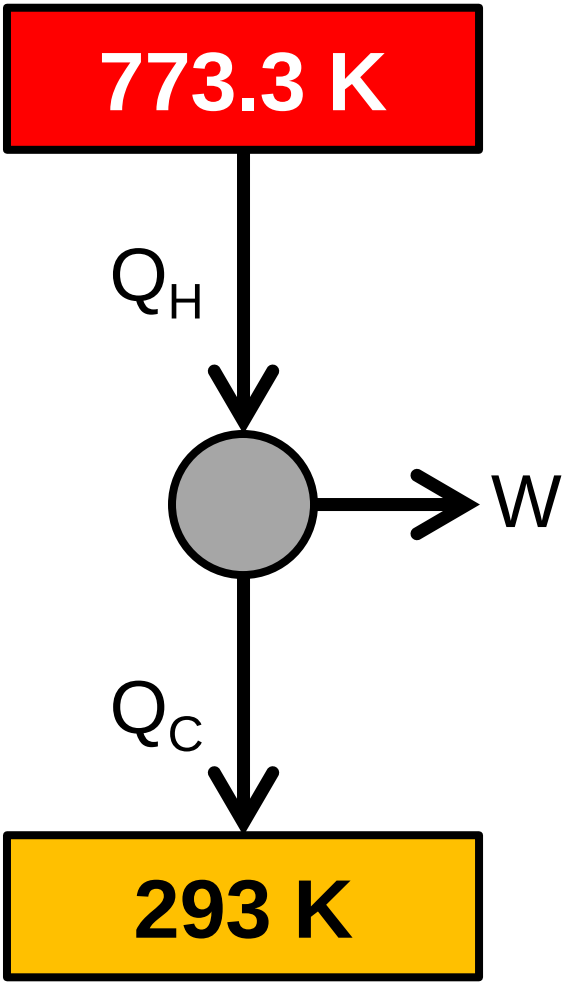

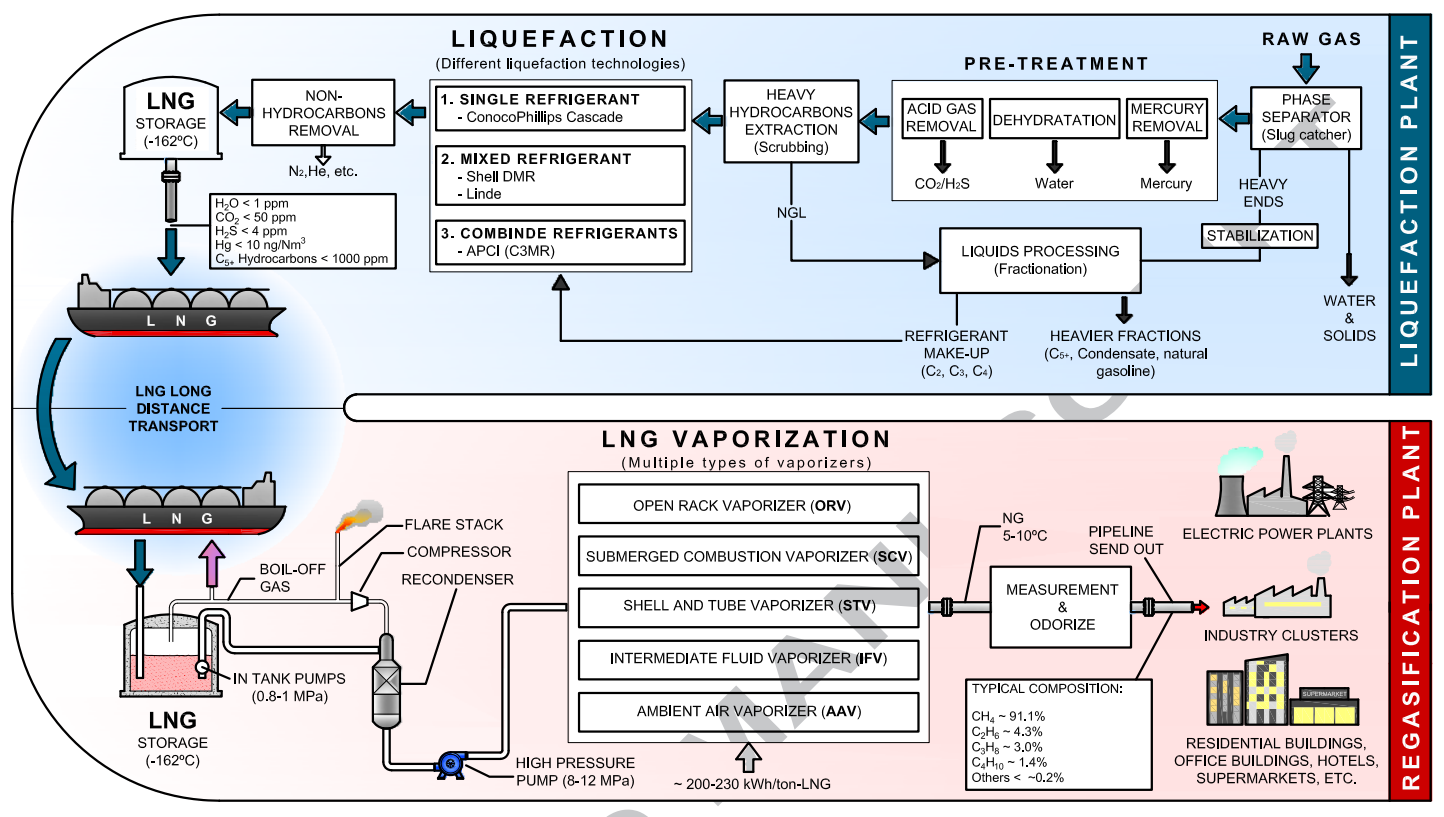
LIQUEFACTION PLANT
LIQUEFACTION
(Different liquefaction technologies)
RAW GAS
PRE-TREATMENT
PHASE SEPARATOR (Slug catcher)
ACID GAS REMOVAL
DEHYDRATATION
MERCURY REMOVAL
CO2/H2S
Water
Mercury
HEAVY HYDROCARBONS EXTRACTION (Scrubbing)
1. SINGLE REFRIGERANT
- ConocoPhillips Cascade
2. MIXED REFRIGERANT
- Shell DMR
- Linde
3. COMBINDE REFRIGERANTS
- APCI (C3MR)
NON-HYDROCARBONS REMOVAL
N2,He, etc.
LNG STORAGE (-162ºC)
H2O < 1 ppm
CO2 < 50 ppm
H2S < 4 ppm
Hg < 10 ng/Nm3
C5+ Hydrocarbons < 1000 ppm
NGL
HEAVY ENDS
STABILIZATION
LIQUIDS PROCESSING (Fractionation)
WATER & SOLIDS
REFRIGERANT MAKE-UP (C2, C3, C4)
HEAVIER FRACTIONS (C5+, Condensate, natural gasoline)
L N G
LNG LONG DISTANCE TRANSPORT
REGASIFICATION PLANT
LNG VAPORIZATION
(Multiple types of vaporizers)
OPEN RACK VAPORIZER (ORV)
SUBMERGED COMBUSTION VAPORIZER (SCV)
SHELL AND TUBE VAPORIZER (STV)
INTERMEDIATE FLUID VAPORIZER (IFV)
AMBIENT AIR VAPORIZER (AAV)
~ 200-230 kWh/ton-LNG
FLARE STACK
COMPRESSOR
RECONDENSER
BOIL-OFF GAS
IN TANK PUMPS (0.8-1 MPa)
HIGH PRESSURE PUMP (8-12 MPa)
LNG STORAGE (-162ºC)
NG 5-10ºC
MEASUREMENT & ODORIZE
PIPELINE SEND OUT
ELECTRIC POWER PLANTS
INDUSTRY CLUSTERS
RESIDENTIAL BUILDINGS, OFFICE BUILDINGS, HOTELS, SUPERMARKETS, ETC.
TYPICAL COMPOSITION:
CH4 ~ 91.1%
C2H6 ~ 4.3%
C3H8 ~ 3.0%
C4H10 ~ 1.4%
Others < ~0.2%

(a) OPEN RACK VAPORIZER (ORV)

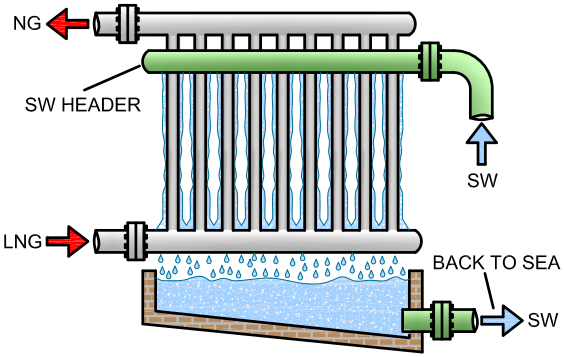

(b) INTERMEDIATE FLUID VAPORIZER (IFV)

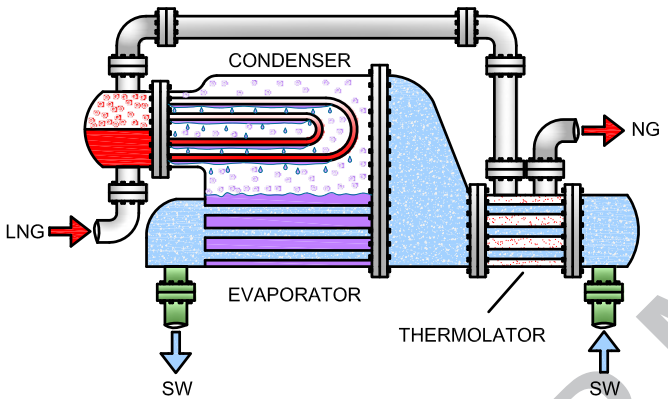

(c) SUBMERGED COMBUSTION VAPORIZER (SCV)

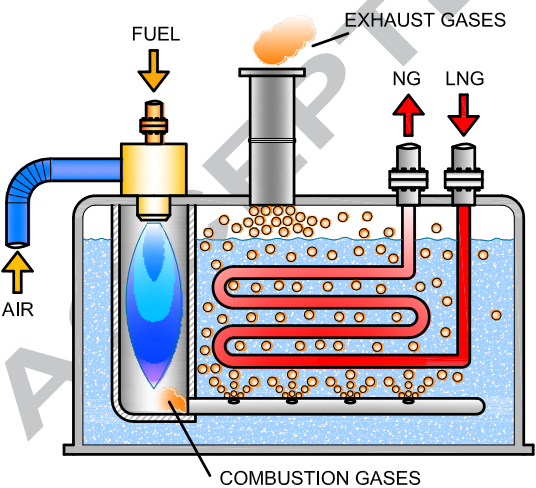

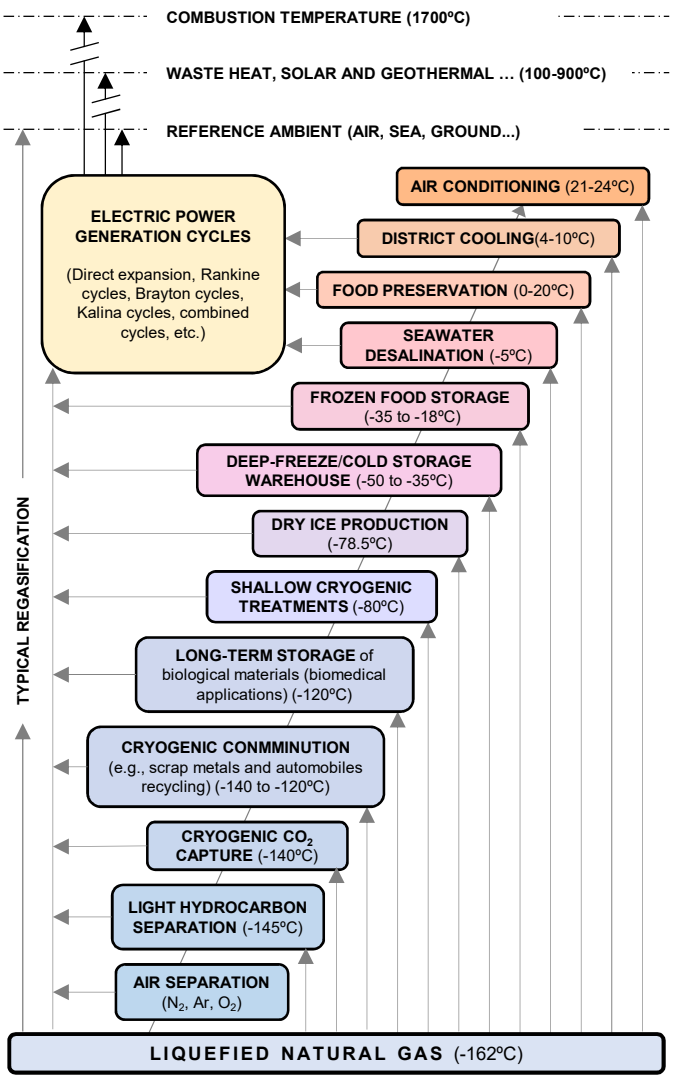
COMBUSTION TEMPERATURE (1700ºC)
WASTE HEAT, SOLAR AND GEOTHERMAL ... (100-900ºC)
REFERENCE AMBIENT (AIR, SEA, GROUND...)
ELECTRIC POWER GENERATION CYCLES
(Direct expansion, Rankine cycles, Brayton cycles, Kalina cycles, combined cycles, etc.)
AIR CONDITIONING (21-24ºC)
DISTRICT COOLING(4-10ºC)
FOOD PRESERVATION (0-20ºC)
SEAWATER DESALINATION (-5ºC)
FROZEN FOOD STORAGE (-35 to -18ºC)
DEEP-FREEZE/COLD STORAGE WAREHOUSE (-50 to -35ºC)
DRY ICE PRODUCTION (-78.5ºC)
SHALLOW CRYOGENIC TREATMENTS (-80ºC)
LONG-TERM STORAGE of biological materials (biomedical applications) (-120ºC)
CRYOGENIC CONMMINUTION (e.g., scrap metals and automobiles recycling) (-140 to -120ºC)
CRYOGENIC CO_2 CAPTURE (-140ºC)
LIGHT HYDROCARBON SEPARATION (-145ºC)
AIR SEPARATION (N_2, Ar, O_2)
TYPICAL REGASIFICATION
LIQUEFIED NATURAL GAS (-162ºC)

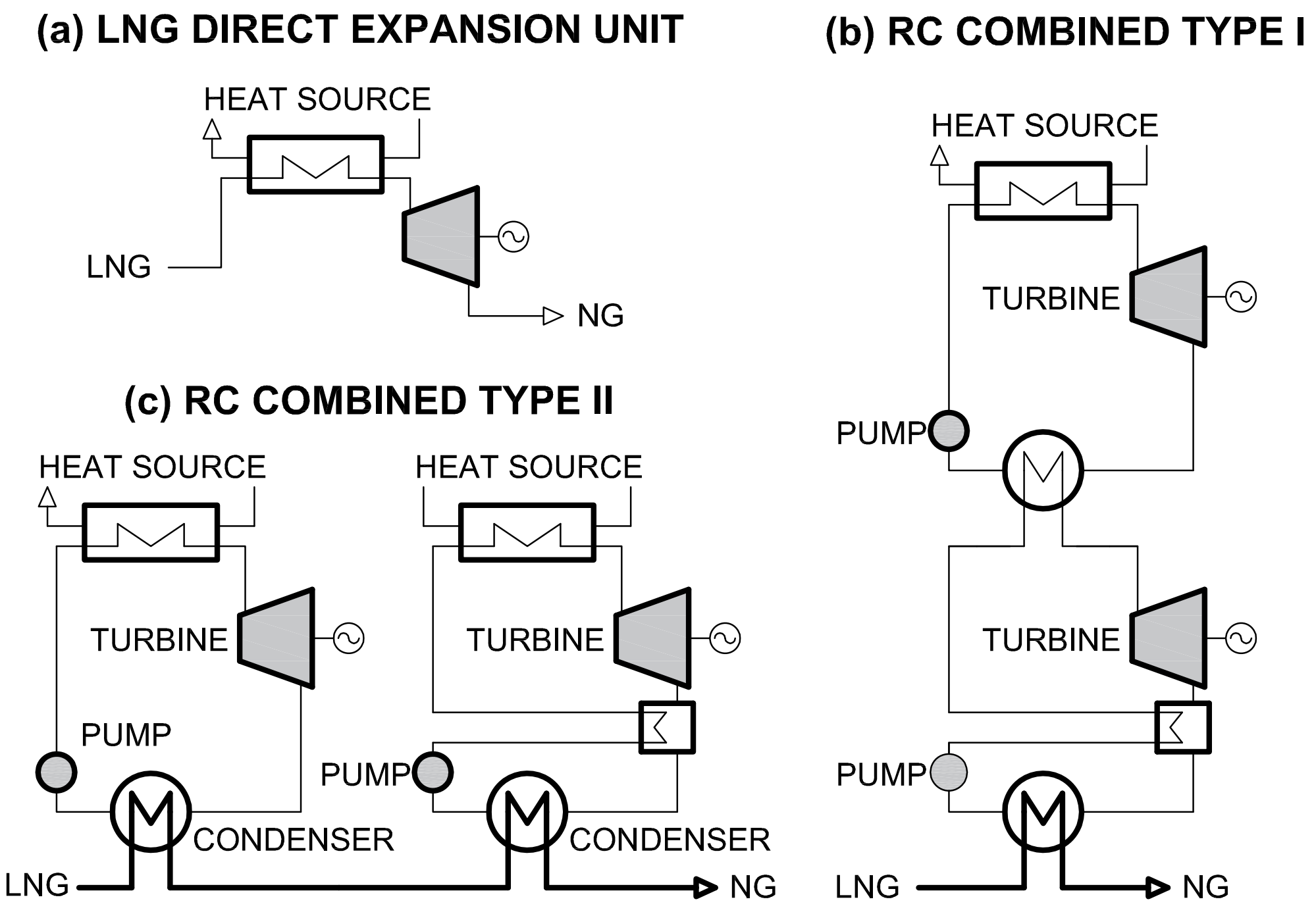
(a) LNG DIRECT EXPANSION UNIT
HEAT SOURCE
LNG
NG
(b) RC COMBINED TYPE I
HEAT SOURCE
TURBINE
PUMP
TURBINE
PUMP
LNG
NG
(c) RC COMBINED TYPE II
HEAT SOURCE
HEAT SOURCE
TURBINE
TURBINE
PUMP
PUMP
CONDENSER
CONDENSER
LNG
NG

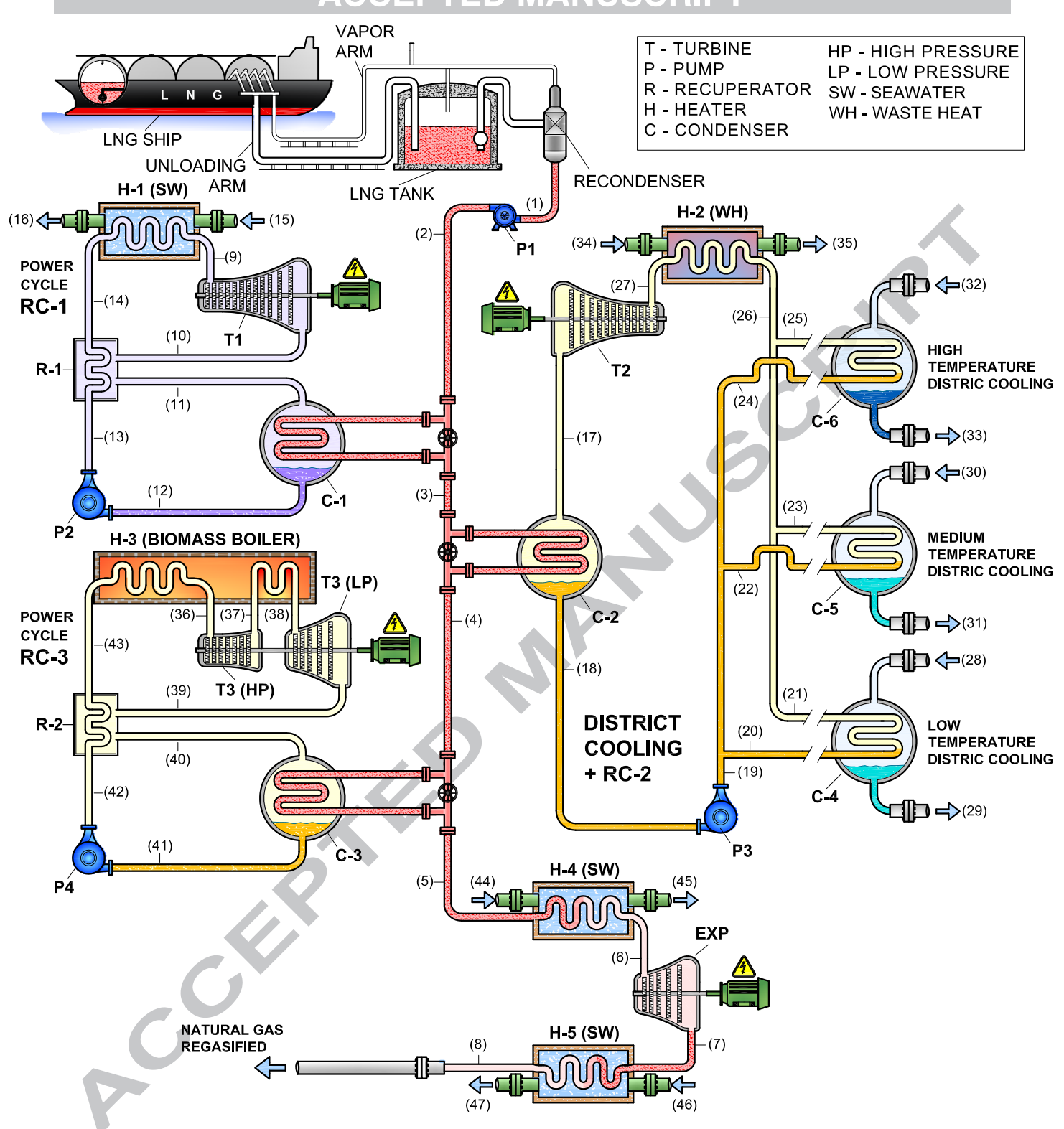

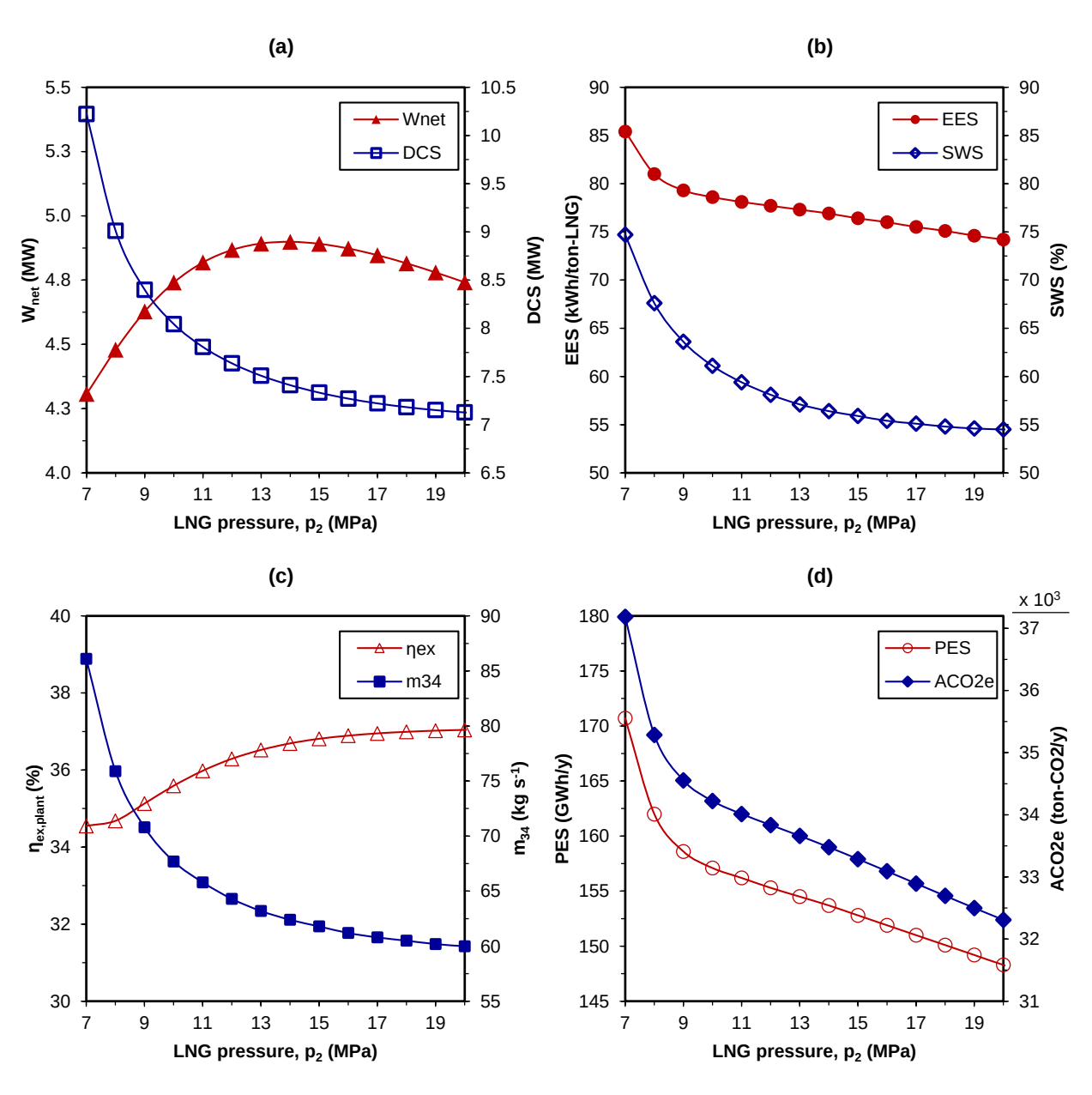
(a)
Wnet
DCS
W_{net} (MW)
DCS (MW)
LNG pressure, p_2 (MPa)
(b)
EES
SWS
EES (kWh/ton-LNG)
SWS (%)
LNG pressure, p_2 (MPa)
(c)
ηex
m34
$\eta_{ex,plant}$ (%)
m_{34} (kg s^{-1})
LNG pressure, p_2 (MPa)
(d)
x 10^3
PES
ACO2e
PES (GWh/y)
ACO2e (ton-CO2/y)
LNG pressure, p_2 (MPa)

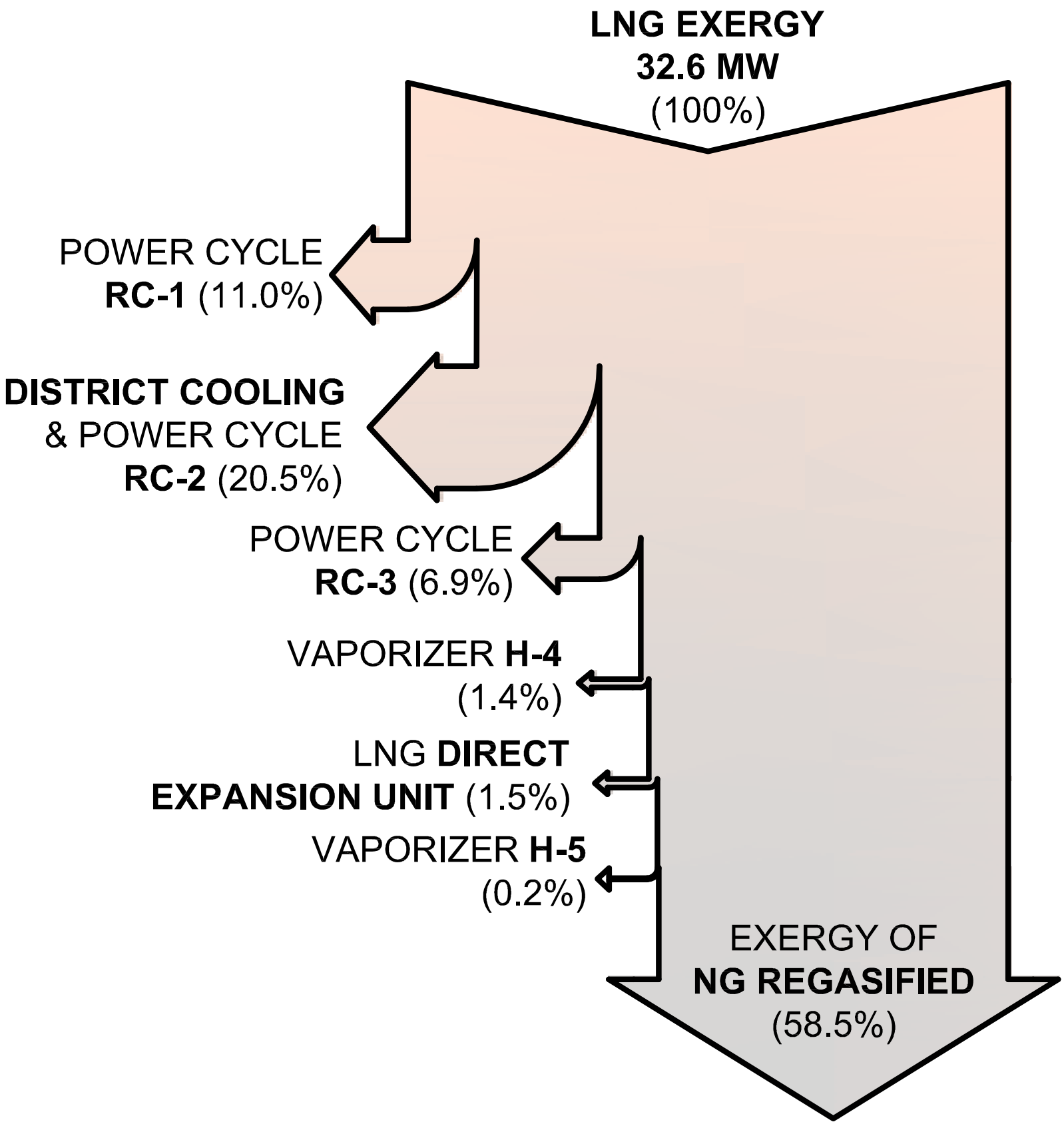
LNG EXERGY
32.6 MW
(100%)
POWER CYCLE
RC-1 (11.0%)
DISTRICT COOLING
& POWER CYCLE
RC-2 (20.5%)
POWER CYCLE
RC-3 (6.9%)
VAPORIZER H-4
(1.4%)
LNG DIRECT
EXPANSION UNIT (1.5%)
VAPORIZER H-5
(0.2%)
EXERGY OF
NG REGASIFIED
(58.5%)

Highlights

- The cold recovery in the LNG regasification is a valuable exergy source.
- Current applications and technologies for LNG cold recovery are reviewed.
- LNG cold can be efficiently exploited via polygeneration.
- A polygeneration plant for cold recovery from LNG-regasification is analyzed.
- An energy saving of 81.1 kWh/ton-LNG and a seawater saving of 67.6% are obtained.